Karl H. Spatschek

Stochastic Transport: Basic Physics for ITER

Why do we need to investigate „anomalous“ transport?
„Fluctuation“ induced transport

„Manageable“ stochasticity: ergodic divertors
Experimental signatures: ELM mitigation, toroidal spin-up, heat flux patterns, runaways
Symplectic field line and drift mappings
Characterization of incomplete chaos
Transport along tangles: Heat flux patterns

Estimates from statistical plasma physics
Ab initio stochastic transport theory for small and large Kubo numbers

HEINRICH HEINE
UNIVERSITÄT
DÜSSELDORF
Institut für Theoretische Physik I

ITER SCHOOL 2007

Need for further basic physics research

There is confidence, based on wide-ranging experience in existing fusion devices, that the fusion performance of ITER will meet the reference target.
However, several key operational aspects remain the subject of focused R&D activities which aim to ensure the reliable operation of the device at or beyond its design capability. … To develop plasma scenarios in which high fusion power production is combined with high confinement and plasma pressure, control of heat and particle fluxes, … the fusion community will need to confront a range of challenges involving plasma physics understanding …
[D.J. Campbell, this meeting]

Performance projections to ITER rely on the H-mode global energy confinement time scaling, since models of local transport … are not yet considered to be sufficiently accurate to replace scaling-based extrapolations.
[D.J. Campbell, Phys. Plasmas 8, 2041 (2001)]

Thermal energy confinement time (s) :

$$\tau_{E,th} = 0.0562\, H_H\, I_p^{0.93}\, B_T^{0.15}\, P^{-0.69}\, n_e^{0.41}\, M^{0.19}\, R^{1.97}\, \varepsilon^{0.58}\, \kappa_a^{0.78} \text{ (rms err. 0.145)}$$

H_H is a factor used to express the degree of enhancement, that might be expected over the current mean prediction (i.e. it is usually 1),

I_p is the plasma current (MA), B_T is the toroidal field on the plasma geometric axis (in T), P is the total net power crossing the separatrix from internal and external sources (MW),

n_e is the geometric mean electron density (10^{19} m^{-3}), M is the atomic mass of the plasma fuel (in AMU), R and a are plasma major and minor horizontal radii (m),

and $\kappa_a = S_o/(\pi a^2)$ with S_o being the plasma cross-sectional area.

Classical transport predictions

Random walk:

Unmagnetized plasma

$$D \equiv \chi_{\|} = \frac{(\Delta \mathrm{x})^2}{2\,\Delta \mathrm{t}} \approx \nu\,\lambda_{\mathrm{mfp}}^2 \approx \frac{\mathrm{v_{th}}^2}{\nu}$$

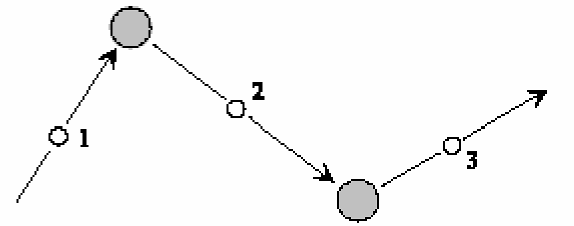

Magnetized plasma

$$D \equiv \chi_{\perp} = \frac{(\Delta \mathrm{x})^2}{2\,\Delta \mathrm{t}} \approx \nu\,\rho_L{}^2 \approx \mathrm{v_{th}}^2\,\frac{\nu}{\Omega_L{}^2}$$

$$\Omega_L = \frac{e\,B}{m\,c}$$

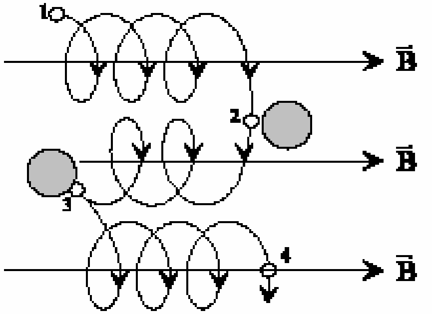

$$\chi_{\perp} = \frac{\nu T c^2}{e^2 B^2} \sim \frac{1}{B^2}$$ magnitude and scaling often not correct!

Kinetic theory and transport truncations

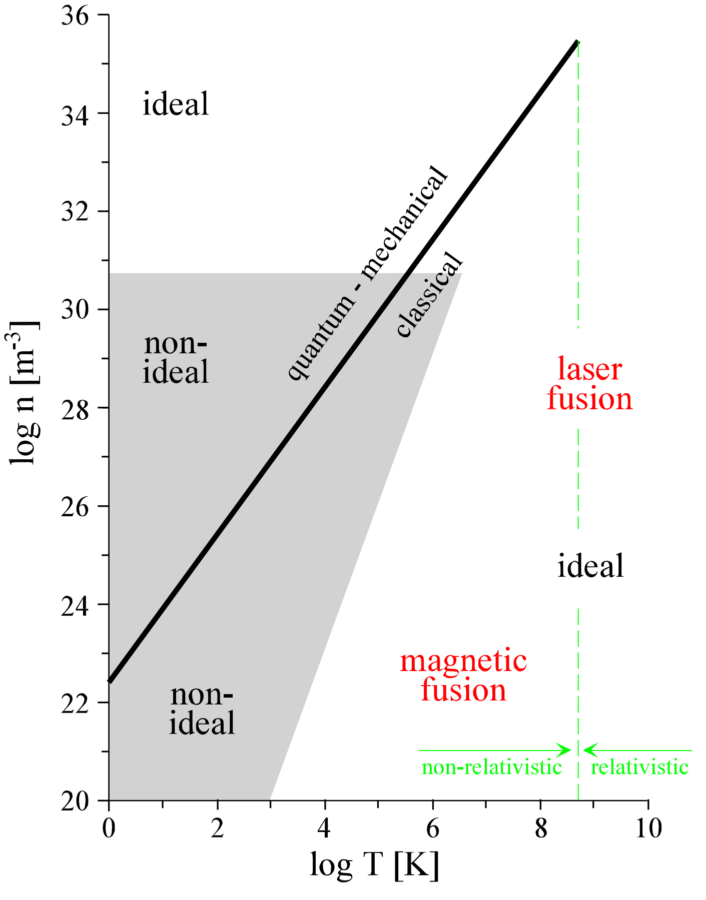

Advantages:

- classical
- non-relativistic
- close to ideal

Disadvantages:

- geometry
- long mean free paths
- many scales
- linear

Kinetic and transport theories

Liouville equation → BBGKY hierarchy
→ truncation(s) in the kinetic regime
→ plasma kinetic equation(s)
(Vlasov, Landau-Fokker-Planck, Balescu-Lenard)
→ averaging over gyromotion
(drift-kinetic, gyro-kinetic equations)

$$\frac{\partial f}{\partial t} + Df = J(f\,|\,f)$$

Kinetic equation → hierarchy of moment equations
→ transport truncations
→ transport equations/coefficients

MHD $\mathrm{u}_{\mathrm{E\times B}} \sim v_{th}$: $f \approx f_M(\vec{v}-\vec{u}) + O(\delta)$, $\delta = \rho / L$

drift $\mathrm{u}_{\mathrm{E\times B}} \sim \delta v_{th}$: $f \approx f_M(\vec{v})\left[1 + 2\frac{u_{||}v_{||}}{v_{th}^2}\right] - \vec{\rho}\cdot\nabla f_M + O(\delta^2)$, $\delta = \rho / L$

Linear transport theory

The classical theory for a homogeneous and stationary magnetic field does not apply as a local theory of transport in a tokamak.
Global geometric characteristics of the confining elements have a strong influence on transport.
Three regimes of collisionality are characteristic of the neoclassical transport theory:
• the banana regime (electronic diffusion increases starting from zero)
• the plateau regime (diffusion almost independent of collisionality)
• the Pfirsch-Schlüter regime (diffusion increases with collisionality)

λ_D Debye length, λ_{mfp} mean free path, $\mathrm{L_H}$ hydrodynamic length, ρ_L Larmor radius

$\lambda_D \ll \rho_L$: Landau type collision term, $\rho_L \ll \mathrm{L_H}$: guiding center transport theory

$\lambda_D \ll \rho_L \ll \lambda_{\mathrm{mfp}} \ll \mathrm{L_H}$: short mean free path regime (collisional regime)

$\lambda_D \ll \rho_L \ll \mathrm{L_H} \ll \lambda_{\mathrm{mfp}}$: long mean free path regime (collisionless regime)

Neoclassical (linear) transport coefficients

Cross-coefficients lead to effects which have no classical or Pfirsch-Schlüter counterparts, e.g.

- a parallel electric field produces an inward radial electron flux
- a parallel electric field produces outward electron and ion heat fluxes
- a parallel electric current is produced by an radial ion heat flux, by a radial electron/ion temperature gradient
- radial pressure gradients may drive (bootstrap) currents

Nevertheless, open problems still exist:

χ_{i} up to a factor 10 different

χ_{e} up to a factor $10 - 10^3$ different

D_a up to a factor 10^2 different

Further demonstration of malfunction of linear transport theory

Magnetic reconnection times

$$\frac{d\vec{B}}{dt} = \frac{\eta c^2}{4\pi}\frac{\partial^2 \vec{B}}{\partial y^2}, \qquad \text{resistive time } \tau_r = \frac{4\pi a^2}{\eta c^2}$$

	Classical resistive time	Observed energy release time
Tokamaks	1 -10 s	100 μs
Solar flares	$10^4\, y$	$20\,\text{min}$
Magnetospheric substorms	∞	$30\,\text{min}$

Problems arise on all scales:

from laboratory experiments (e.g. L $\sim 10^2\, \rho_i$) [electron and ion losses]

up to galaktic discs (d $\sim\; 10^{27}\, \rho,\;\; \rho \sim 1$ AU) [cosmic radiation]

Nonlinear transport

$$\partial_t \vec{\Gamma} = -\nabla \cdot (\vec{u}\,\vec{\Gamma}) - \nabla P - \nabla \cdot \overleftrightarrow{\Pi} + \frac{e}{mc}\vec{\Gamma} \times \vec{B} + \frac{e}{m}\vec{E} + \frac{1}{m}\vec{R}$$

$$X := \langle X \rangle + \delta X$$

classical

neo-classical

$$\langle \Gamma_x \rangle = \frac{1}{m\Omega}\langle R_y \rangle + \frac{1}{\Omega}\langle (\hat{b} \times \nabla \cdot \overleftrightarrow{\Pi}) \cdot \hat{x} \rangle + \Gamma_x^{anomalous} + \Gamma_x^{time-dependent}$$

$$\Gamma_x^{anomalous} = \frac{c}{B}\langle \delta n\, \delta E_y \rangle + \frac{1}{B}\left\{ \langle \delta\Gamma_{\parallel}\, \delta B_x \rangle - \langle \delta\Gamma_x\, \delta B_{\parallel} \rangle \right\}$$

Nonlinear gyrokinetics → advanced computation

Advances in Computational Plasma Physics

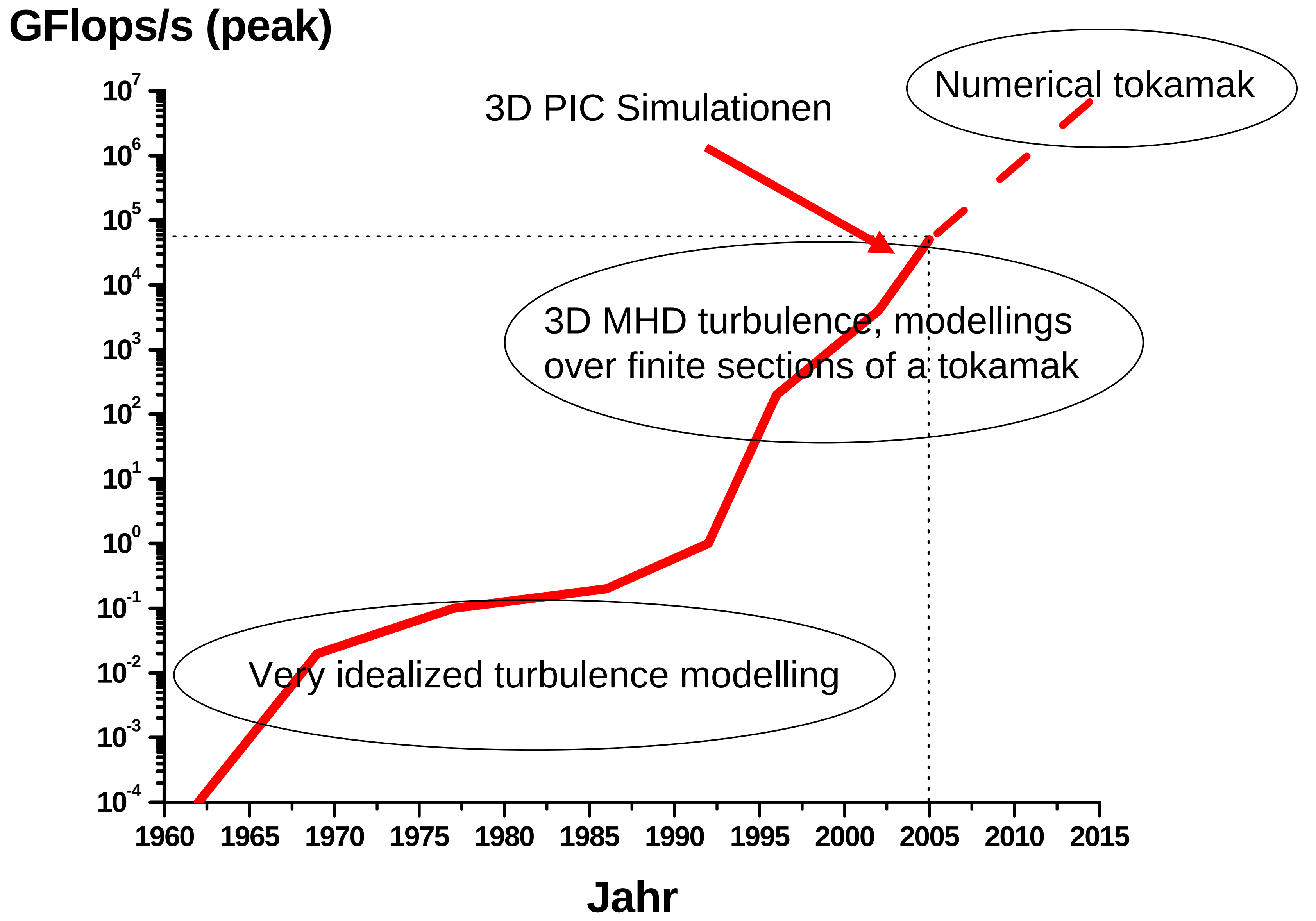

Analytical Approaches

Weak Turbulence Theory

$\dot{\Psi} = L\Psi + \frac{1}{2}M\Psi\Psi$, $L = i\Omega - \gamma$, characteristic frequency Ω

$C_2(t,t') = \langle \delta\Psi(t)\delta\Psi(t') \rangle$ [correlation function]

Multiple scale analysis, $\Omega_{\vec{k}} + \Omega_{\vec{p}} + \Omega_{\vec{q}} \equiv \Delta\Omega$, $\vec{k} + \vec{p} + \vec{q} = 0$

$$\left(\frac{\partial}{\partial t_1} - 2\gamma \right) C_2 = M^2 \delta(\Delta\Omega) C_2^2$$

Fluctuation spectrum: $\langle \delta\varphi_k \delta\varphi^*_{k'} \rangle = n(k,t)\delta(k-k')$

Wave kinetic equation: $\dfrac{\partial n(k,t)}{\partial t} = I(k,t) + \Gamma(k)n(k,t)$

The closure problem, renormalization, and structures

In reality, the resonance is broadened

- terms through all orders are required
- renormalization is required

→ strong turbulence theory

DIA (Direct Interaction Approximation) closure
EDQNM (Eddy Damped Quasi-Normal Markovian) closure
RMC (Realizable Markovian Closure)
…

Coherent structures

Zonal flows
Blob generation in a turbulent tokamak edge
…

Intermittency

Scaling Laws

Continuity equation in k-space $\frac{\partial E(k)}{\partial t}+\frac{\partial P(k)}{\partial k}=0$

$$[E]=\left[\frac{gL^2}{T^2}\right] \qquad [E(k)]=\left[\frac{\rho L^{6-d}}{T^2}\right]$$

$$[\rho]=\left[\frac{g}{L^3}\right] \qquad [P(k)]=\left[\frac{\rho L^{5-d}}{T^3}\right]$$

fluid turbulence: $[E(k)]=\left[\frac{\rho L^{6-d}}{T^2}\right]\sim \rho^{1/3}P^{2/3}k^{d/3-8/3}\sim k^{-5/3}$ (Kolmogorov)

plasma turbulence: $[\omega=\omega(\mathrm{k})]=\left[\frac{1}{T}\right]\rightarrow$ non-dimensional variable $\xi=\frac{Pk^{5-d}}{\rho\omega^3}$

$E(k)\sim\rho\omega^2(k)k^{d-6}f(\xi)\rightarrow$ more freedom!

e.g. $f(\xi)\sim\xi^{1/3}$

Heuristic methods (small scale fluctuations)

$$\Gamma_r \approx \langle \delta n \, \delta u_r \rangle \triangleq -D \frac{\langle n \rangle}{L_n} \quad \text{[electrostatic turbulence]}$$

$$\frac{\gamma_{\mathrm{k}}}{\omega_{\mathrm{k}}} \sim \delta_k \,, \quad \omega_{\mathrm{k}} \approx \frac{ckT}{eBL_n} \,, \quad \delta n_k \approx \langle n \rangle \frac{e\phi_k (1 - i\delta_k)}{T} \,, \quad \delta u_r \approx ick \frac{\phi_k}{B} \quad \text{[drift wave]}$$

$$\Gamma_r \approx \langle n \rangle \frac{cT}{eB} \sum_k k\delta_k \left| \frac{\delta n_k}{\langle n \rangle} \right|^2$$

$$\nabla \, \delta n \triangleq ik\delta n_k \sim \frac{\langle n \rangle}{L_n} \quad \text{[saturation]}$$

$$\boxed{\mathrm{D} \approx \frac{\gamma_{\max}}{k_{\max}^2}}$$

Mixing length argument (Prandtl)

$$\boxed{D \approx \frac{L_r^2}{\tau_c}}$$

L_r mode radial correlation length, τ_c autocorrelation time for turbulent fields

small scale turbulence: $L_r \approx \rho_s \sim \rho_i$ [thermal ion Larmor radius]

$$\tau_c^{-1} \approx \omega_T^* \equiv \frac{k_\Theta T}{BL_T} \sim \frac{v_{ti}}{a} \text{ [diamagnetic frequency] }, \; k_\Theta \approx \rho_i^{-1}$$

$$\boxed{D \sim \rho_i^2 \omega_T^* \sim D_{Bohm} \frac{\rho^*}{L_T^*} \sim \mathrm{T}^{3/2}\mathrm{B}^{-2} \quad \text{[gyro-Bohm]}}$$

large scale turbulence: e.g. $L_r \approx \sqrt{a\rho_s}$ through self-organization

$$\boxed{D \sim \rho_i v_{ti} \sim D_{Bohm}\left[\frac{\mathrm{m}^2}{\mathrm{s}}\right] = \frac{\mathrm{T[eV]}}{16\,\mathrm{B[T]}} \sim \mathrm{T}\,\mathrm{B}^{-1} \quad \text{[Bohm]}}$$

e.g. gyro-Bohm in H-Mode, Bohm or Goldstone regime $D \sim \rho_i^{1/2}$ in L-Mode

Self-organization conjecture

Let a system be modeled by a nonlinear partial differential equation, with dissipation, for the field u. The system contains (at least) two quadratic or higher-order conserved quantities in the absence of dissipation. One of the conserved quantities, let us say $A(u)$, decays faster than the other(s), e.g. $B(u)$. The modal cascade in the quantity B is towards small wave-numbers. Then, the field is expected to reach a quasi-stationary state which minimizes A for constant B, i.e.

$$\delta A - \lambda \delta B = 0$$

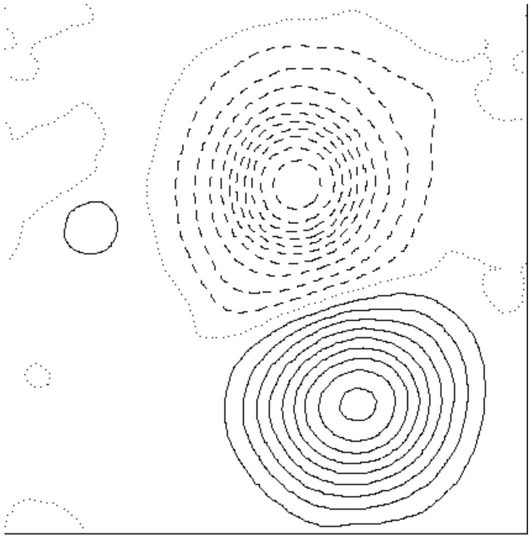

$t = 400 \quad dz = 120$

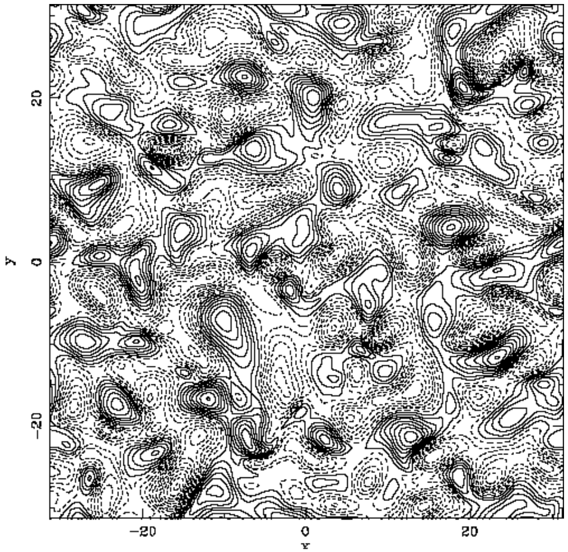

Effective parallel transport in the presence of magnetic fluctuations

$$\frac{\partial T}{\partial t} = \kappa_{\|} \left(\hat{n} \cdot \nabla\right)^2 T$$

$$\hat{n}_0 \equiv \frac{\vec{B}_0}{B_0} \quad , \qquad \kappa_{\|} = \frac{\mathrm{v}_{th}^2}{\nu} \gg \kappa_{\perp}$$

$$\vec{B} = \vec{B}_0 + \delta\vec{B} \quad , \qquad \vec{b} = \frac{\delta\vec{B}}{B}$$

$$\frac{\partial\langle T\rangle}{\partial t} = \kappa_{\|}\langle b^2\rangle \frac{\partial^2\langle T\rangle}{\partial x_{\perp}^2} + \kappa_{\|}\left\langle b\frac{d}{dx_{\perp}}\left(\hat{n}_0 \cdot \nabla\right)\delta T\right\rangle$$

effective parallel transport

Status of analytical turbulence predictions

Self-consistent models

- are generally very difficult to solve
- are often good for scaling arguments

Heuristic models

- are often ad hoc
- are good for rough interpretations
- are, strictly speaking, not predictive

Non-locality, intermittency, interaction with coherent structures, …
are open problems

„Manageable“ stochasticity

„Old“ paradigm: Stochasticity is

- mainly caused by plasma instabilities in high-dimensional phase space
- always counter-productive, i.e. enhanced losses

(micro-instabilities, MHD instabilities, ripple losss, …
due to thermodynamic forces and currents)

Nonlinear dynamics: Already a few degrees of freedom system may become stochastic

(Field-errors due to confinement, heating, shaping and correction coils,
MHD control coils (RWM) and boundary layer coils, Ergodic divertor coils, …)

„New“ paradigm: Stochastization may have positive aspects

- manageable in some respect
- ELM mitigation, particle exhaust, zonal flows, …

Tore-Supra, Island divertor in stellarators, DIII-D, Textor, JET (ASDEX-U, ITER): external sources for magnetic fluctuations

TORE SUPRA

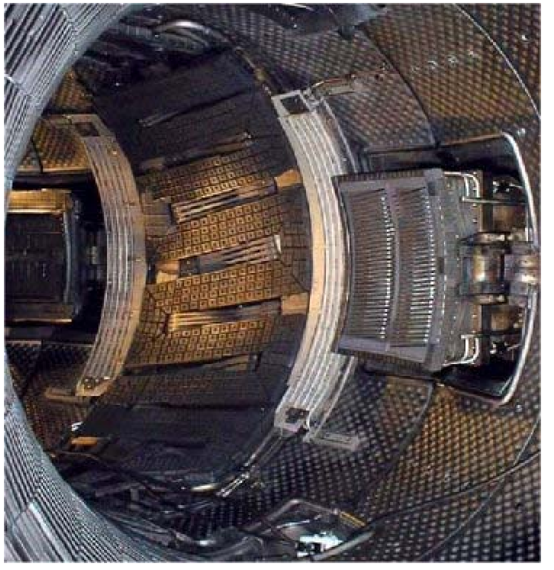

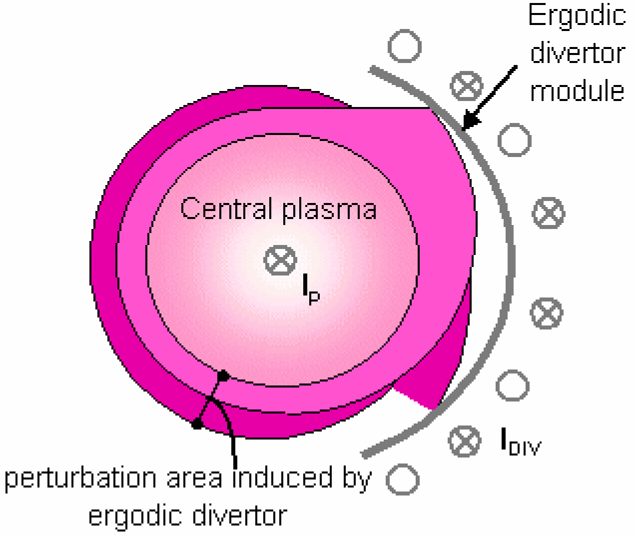
Ergodic
divertor
module
Central plasma
I_P
I_{DIV}
perturbation area induced by
ergodic divertor

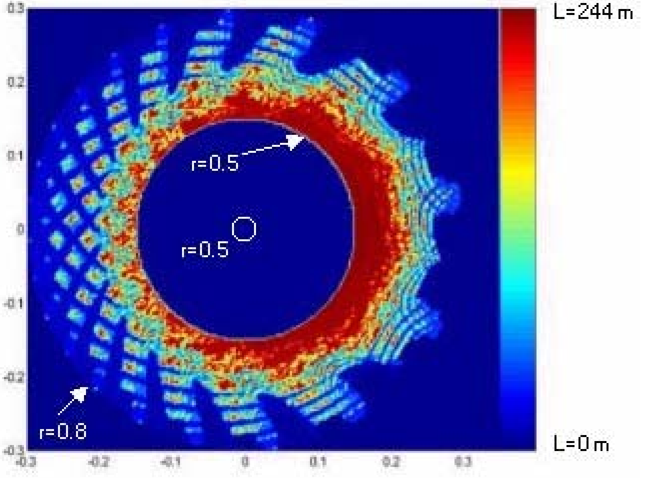
L=244 m
L=0 m
r=0.5
r=0.5
r=0.8
0.3
0.2
0.1
0
-0.1
-0.2
-0.3
-0.3
-0.2
-0.1
0
0.1
0.2
0.3

DIII-D configuration

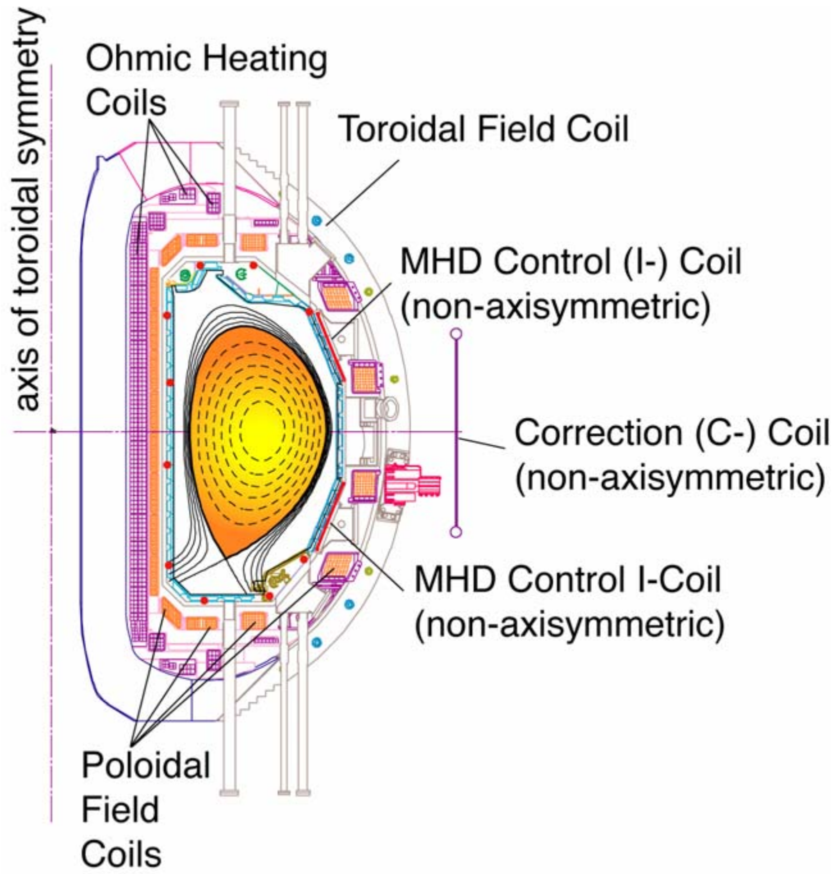

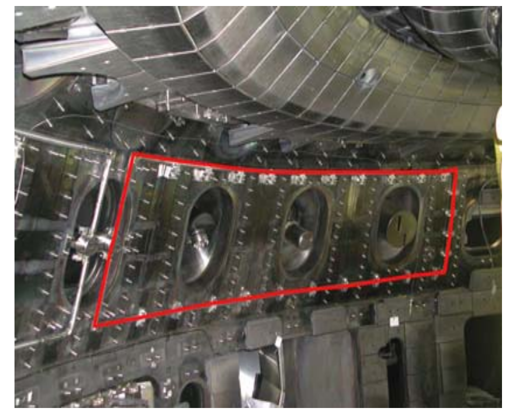

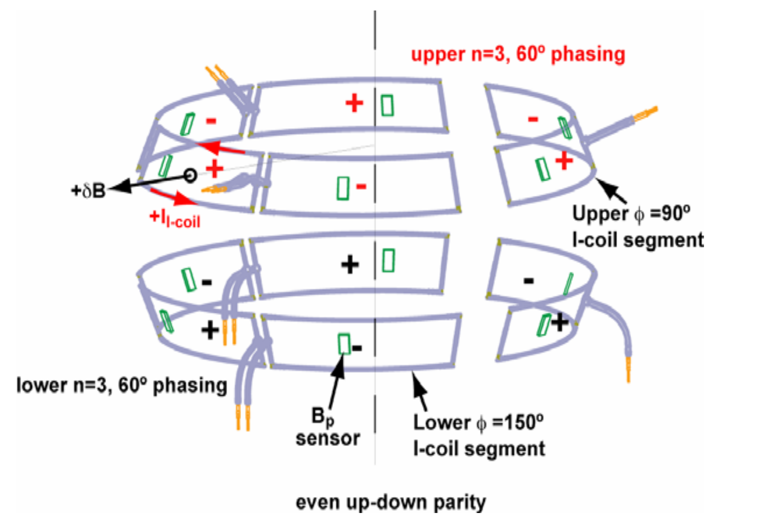

TEXTOR

A unique feature of TEXTOR is the Dynamic Ergodic Divertor (DED).
This device consists of a set of 16 helical coils mounted on the high-field side of the torus inside the vacuum vessel.
The coils can be connected to produce perturbation fields with the fundamental mode numbers m/n = 12/4, 6/2, and 3/1.
The coils can be supplied with dc current yielding a static perturbation field, or with ac currents resulting in a rotating field.
The frequency of the rotating perturbation field can be either low (~ 50 Hz) or high frequency in the range 1 kHz to 10 kHz.
These frequencies are of the order of the electron diamagnetic drift frequency for TEXTOR discharge conditions.
The maximum coil current depends on the frequency and can be up to 15 kA.

Becoulet (2007)

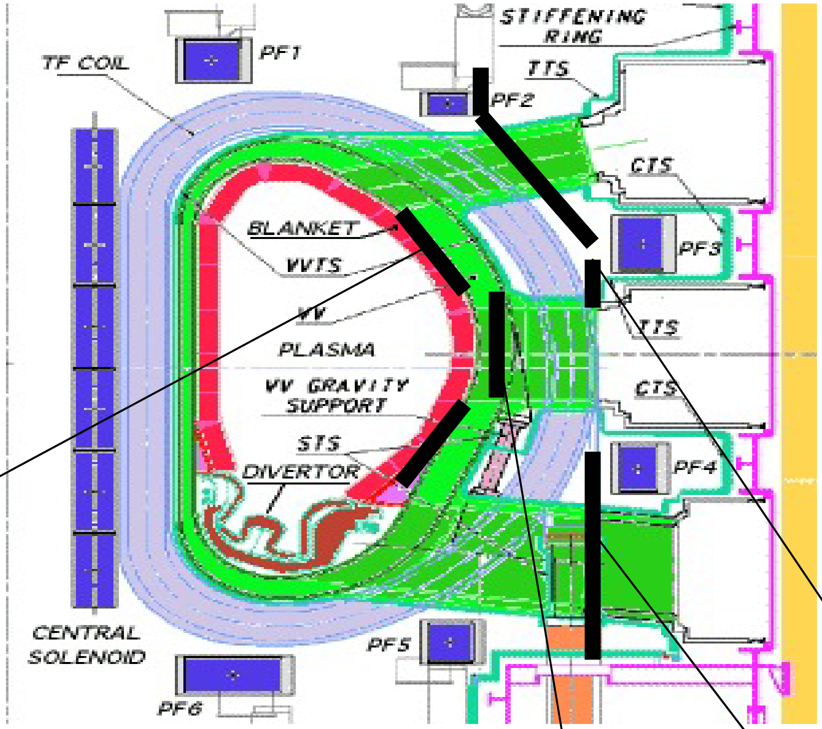

Larger current,but better accessibility!

Blanket coils:2*6*(5+5): 20kA/11turns

9 mid-ports coils: 150kA/11turns

36 external coils: 200-300kA

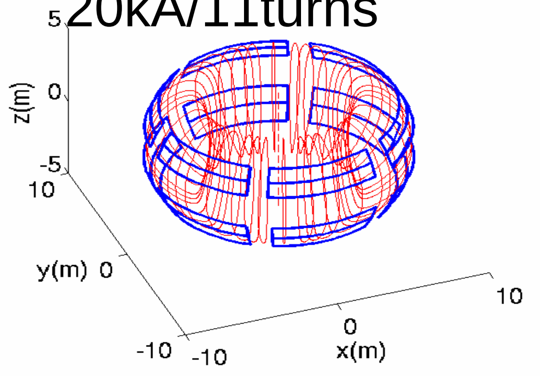

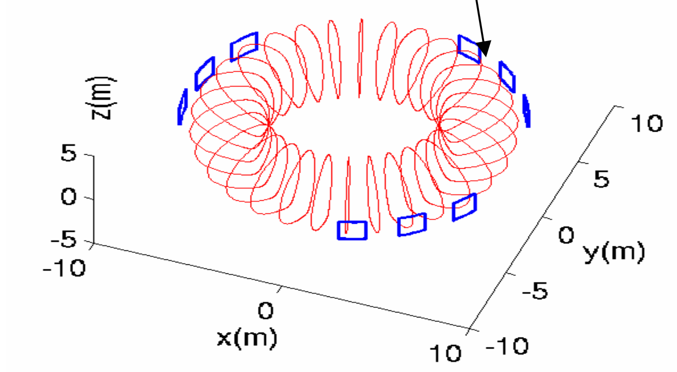

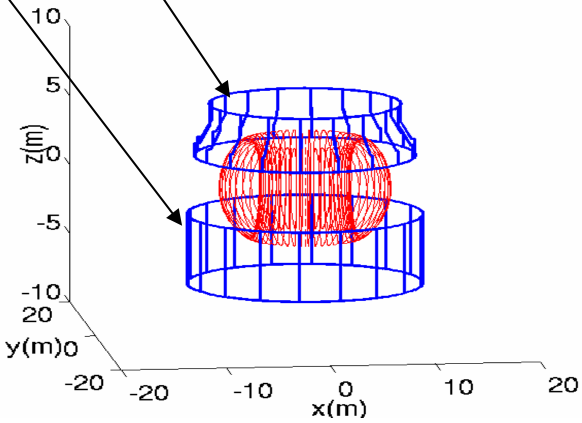

DIII-D results

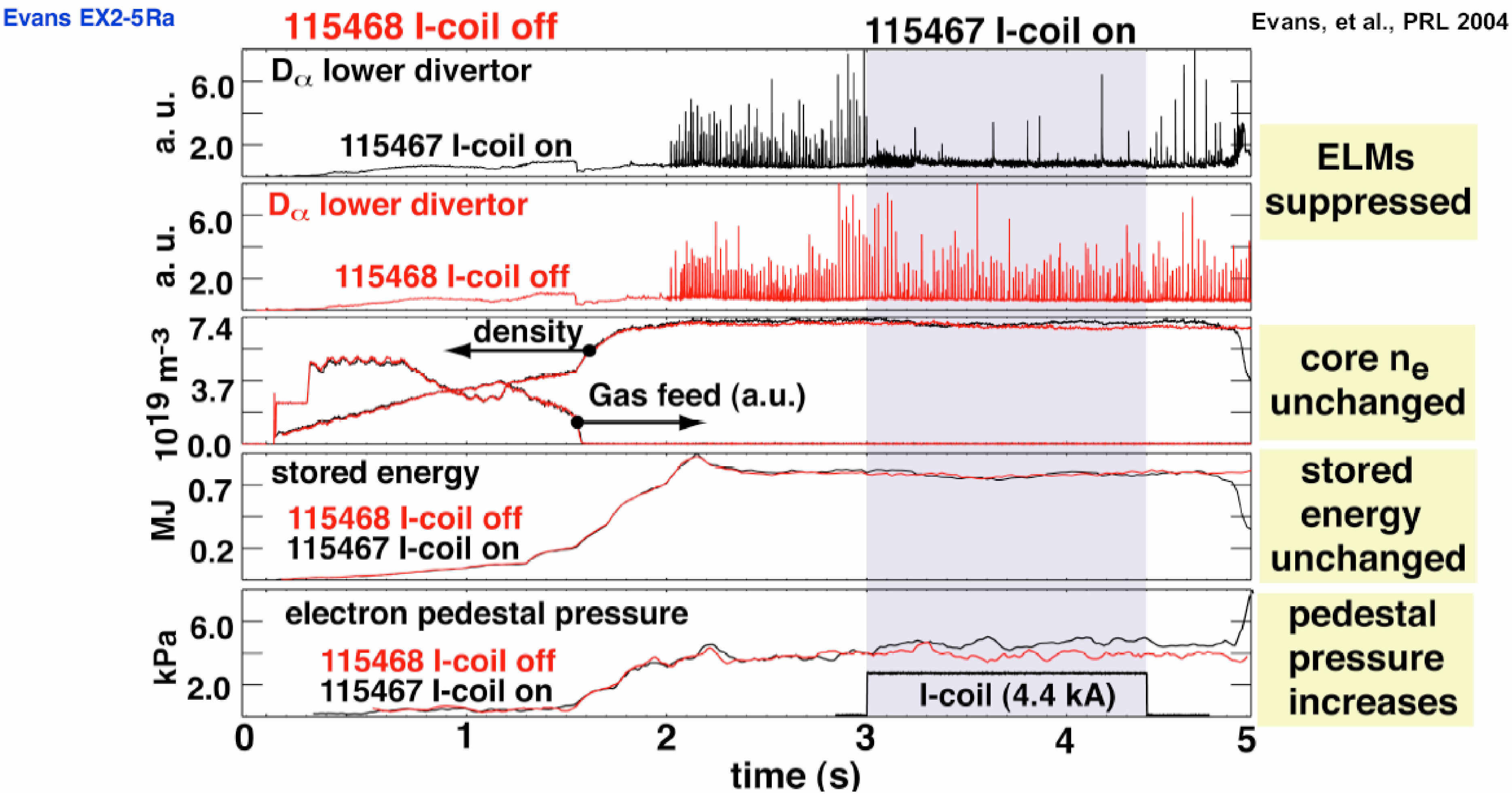

Type-I ELMs are suppressed with resonant magnetic perturbations

Toroidal spin-up of the plasma in TEXTOR (m/n=3/1)

$$\omega_\phi = \frac{v_\phi}{R}$$

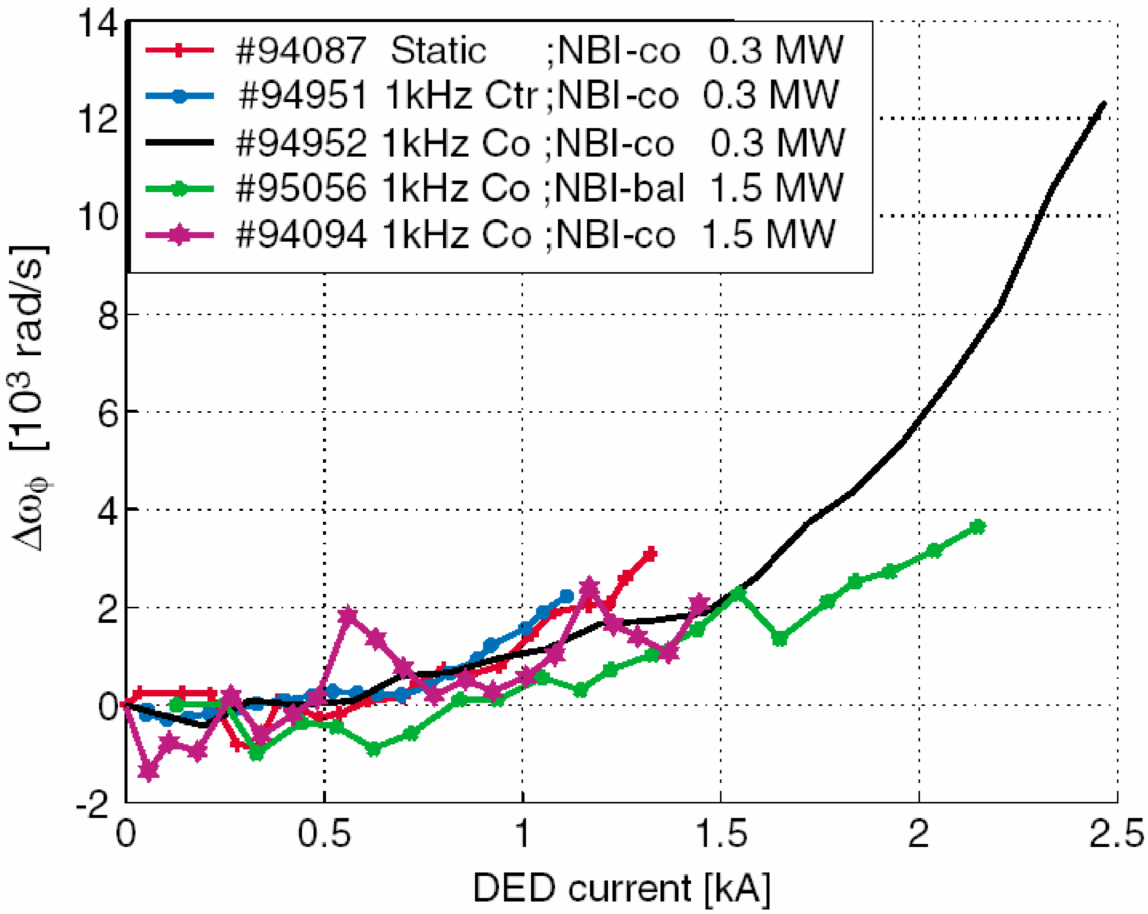

$$E_r \leftrightarrow v_\phi \times B_\theta$$

Finken et al, PRL 2005

Runaway escape rates

slow (appr. 5 MeV)

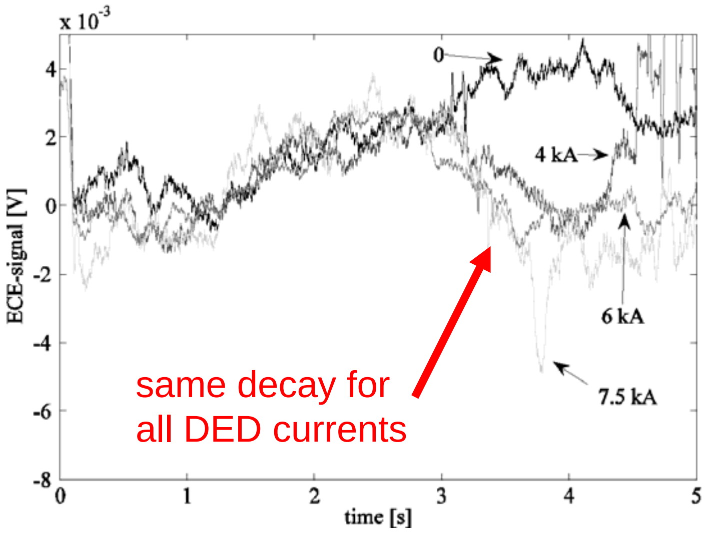

fast (appr. 25-30 MeV)

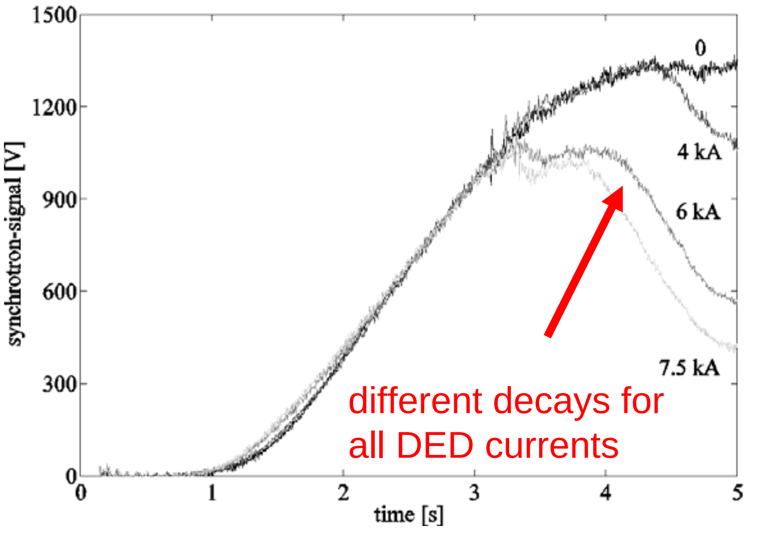

$$N(t) \approx N_0 \left(N_1 + \exp\{-\lambda t\} \right)$$

$$\lambda \sim -(E - E_c)$$

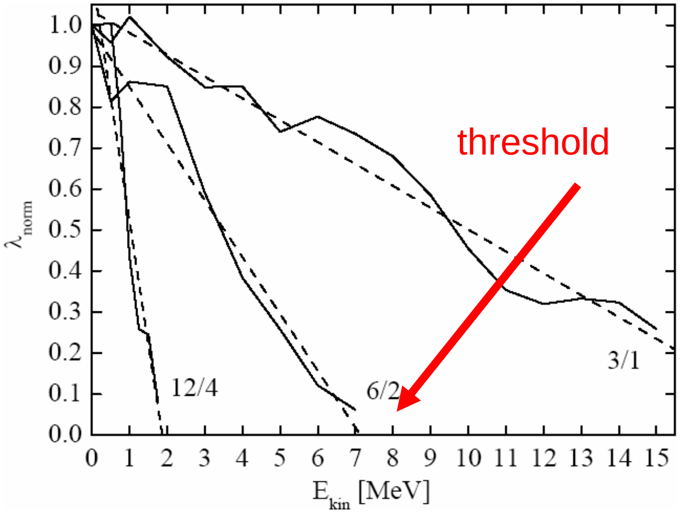

Heat flux patterns (TEXTOR [top], DIII-D [bottom])

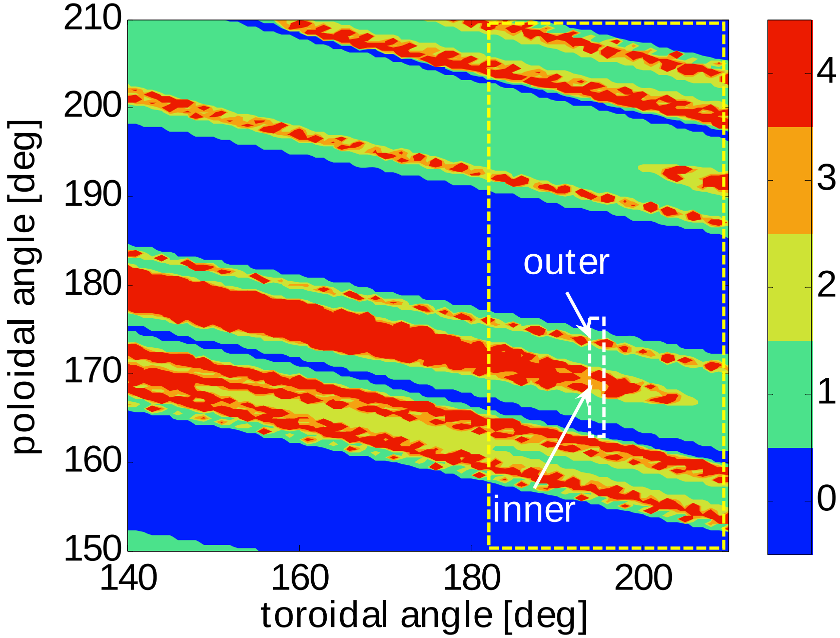

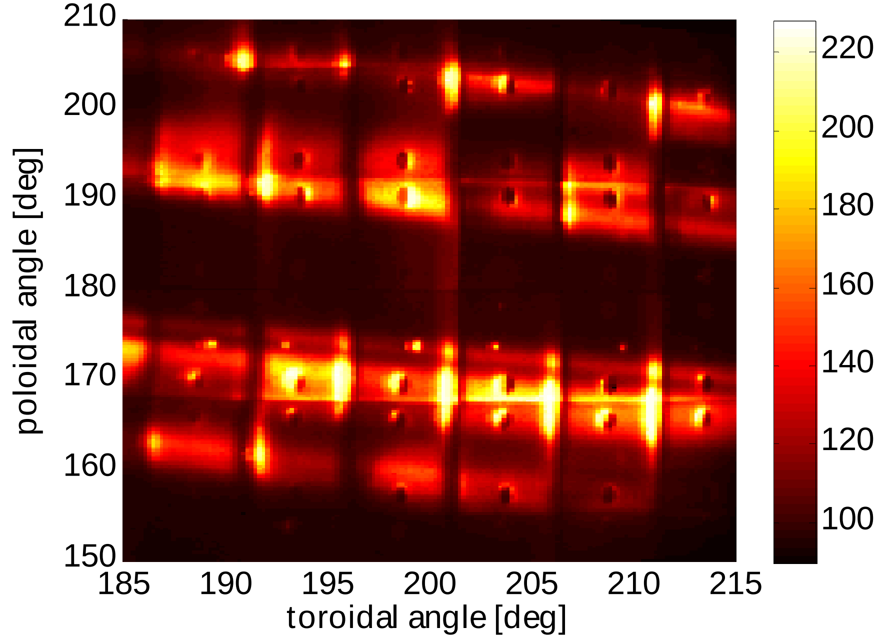

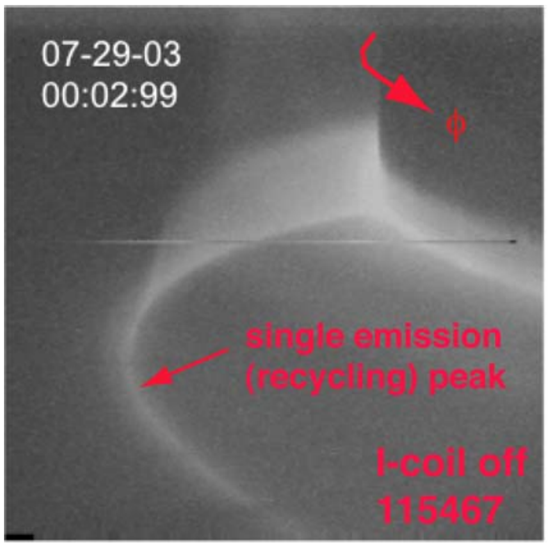

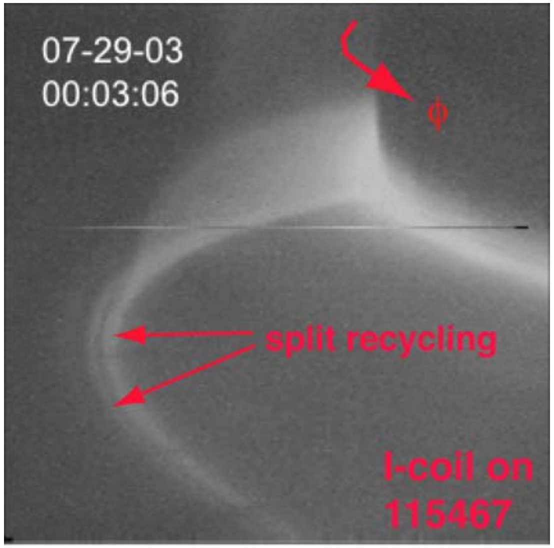

Semi-analytical treatments

$$\vec{B} = \nabla\psi \times \nabla\theta - \nabla\Psi_p \times \nabla\varphi \quad \text{[Clebsch Representation]}$$

$$\vec{B} = \nabla \times \vec{A} \;,\quad \vec{A} = A_\rho \nabla\rho + A_\theta \nabla\theta + A_\zeta \nabla\zeta \;,\quad \frac{\partial G(\rho,\theta,\zeta)}{\partial\rho} := A_\rho$$

$$\psi = A_\theta - \frac{\partial G(\rho,\theta,\zeta)}{\partial\theta} \;,\quad -\psi_p = A_\zeta - \frac{\partial G(\rho,\theta,\zeta)}{\partial\zeta}$$

$$\Psi_p \equiv H = \int \frac{d\psi}{q(\psi)}$$

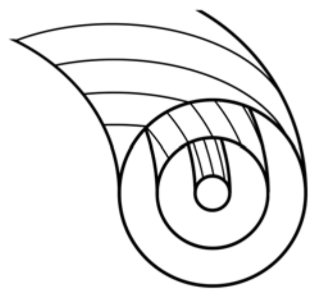

$$\Psi_p \equiv H = \int \frac{d\psi}{q(\psi)} + H_1(\psi,\theta,\varphi)$$

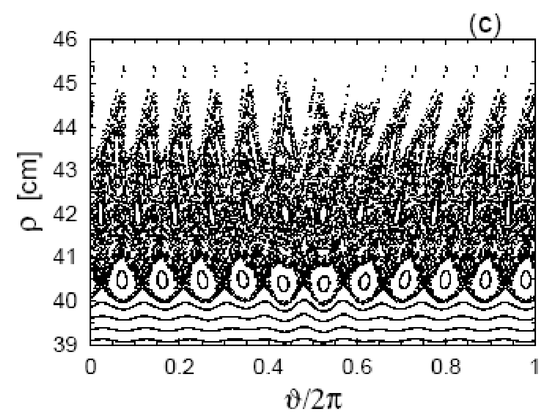

Hamiltonian system

$$\vec{B} = \nabla\psi \times \nabla\theta - \nabla H \times \nabla\varphi$$

$$\begin{aligned}
d\psi &= \vec{B}\cdot\nabla\psi = -(\nabla H \times \nabla\varphi)\cdot\nabla\psi \\
&= -(\frac{\partial H}{\partial\theta}\nabla\theta \times \nabla\varphi)\cdot\nabla\psi = -\frac{\partial H}{\partial\theta}(\nabla\psi \times \nabla\theta)\cdot\nabla\varphi \\
d\theta &= \vec{B}\cdot\nabla\theta = -(\nabla H \times \nabla\varphi)\cdot\nabla\theta \\
&= -(\frac{\partial H}{\partial\psi}\nabla\psi \times \nabla\varphi)\cdot\nabla\theta = \frac{\partial H}{\partial\psi}(\nabla\psi \times \nabla\theta)\cdot\nabla\varphi \\
d\varphi &= \vec{B}\cdot\nabla\varphi = (\nabla\psi \times \nabla\theta)\cdot\nabla\varphi
\end{aligned}$$

$\Longrightarrow$ Hamiltonian equations of motion

$$\frac{d\psi}{d\varphi} = -\frac{\partial H}{\partial\theta} \qquad \frac{d\theta}{d\varphi} = \frac{\partial H}{\partial\psi}$$

Resonances

$$H(\vec{J},\vec{\theta}) = H_0(\vec{J}) + \delta H(\vec{J},\vec{\theta})$$

$$\frac{\partial H}{\partial \vec{J}} = \dot{\vec{\theta}} = \vec{\Omega}(\vec{J}) + \frac{\partial \delta H}{\partial \vec{J}} \ , \quad \frac{\partial H}{\partial \vec{\theta}} = -\dot{\vec{J}} = \frac{\partial \delta H}{\partial \vec{\theta}}$$

$$\delta H(\vec{J},\vec{\theta}) = \sum_{\vec{m}} e^{i\vec{m}\cdot\vec{\theta}} H_{\vec{m}} \ , \quad \vec{\theta} \approx \vec{\theta}_0 + \vec{\Omega} t$$

$$\Delta \vec{J} = -\int dt \frac{\partial \delta H}{\partial \vec{\theta}} \approx -i \sum_{\vec{m}} \frac{\vec{m} H_{\vec{m}} e^{i\vec{m}\cdot\vec{\theta}_0} \left(e^{i\vec{m}\cdot\vec{\Omega} t} - 1 \right)}{\vec{m}\cdot\vec{\Omega}}$$

$\vec{m}\cdot\vec{\Omega}(\vec{J}) = 0$ [resonances]

Resonances, Chirikov overlap criterion, butterfly effect

Perturbation terms $\varepsilon H_{mn}(\psi)\cos(m\vartheta + n\varphi + \chi_{m0})$

are resonant on the rational magnetic surfaces ψ_{mn}

with $q(\psi_{mn}) = m/n \rightarrow$ creating a chain of islands

$$\mathrm{W}_{\mathrm{mn}} = 4\left|\frac{\varepsilon H_{mn}(\psi_{mn})}{dq^{-1}/d\psi}\right|^{1/2} \quad \text{[island width]}$$

$$\sigma_{\mathrm{Chir}} = \frac{W_{mn} + W_{m+1n}}{2\left|\psi_{m+1n} - \psi_{mn}\right|} \geq 1 \quad \text{[Chirikov parameter} \rightarrow \text{onset of chaos]}$$

TEXTOR DED:

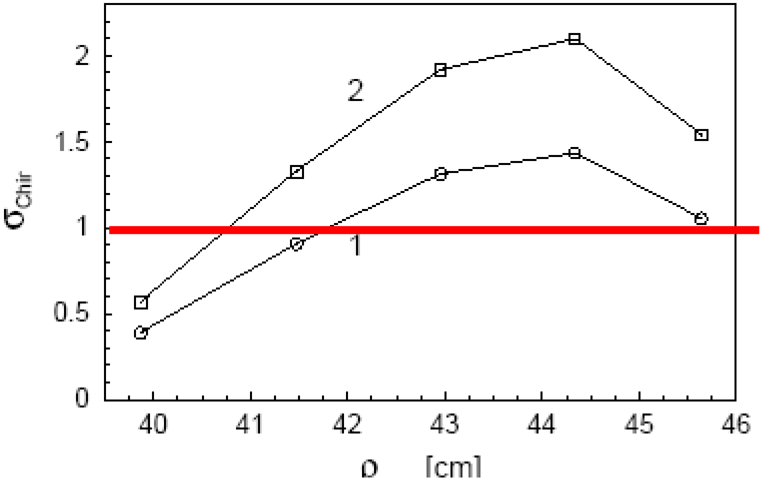

Symplectic Mapping

The conventional method to determine the magnetic field topology is numerical field line tracing, but symplectic mappings are faster!

$$(\vartheta_{k+1},\psi_{k+1}) = \hat{M}(\vartheta_k,\psi_k)$$

$$S_k = S(\vartheta,\Psi,\varphi;\varepsilon)\Big|_{\varphi=\varphi_k}$$

$$\Psi_k = \psi_k - \varepsilon\frac{\partial S_k}{\partial\vartheta_k}, \qquad \Theta_k = \vartheta_k + \varepsilon\frac{\partial S_k}{\partial\Psi_k}$$

$$\Psi_{k+1} = \Psi_k, \qquad \Theta_{k+1} = \Theta_k + \frac{(\varphi_{k+1}-\varphi_{k+1})}{q(\Psi_k)},$$

$$\psi_{k+1} = \Psi_{k+1} + \varepsilon\frac{\partial S_{k+1}}{\partial\vartheta_{k+1}}, \qquad \vartheta_k = \Theta_{k+1} - \varepsilon\frac{\partial S_{k+1}}{\partial\Psi_{k+1}}$$

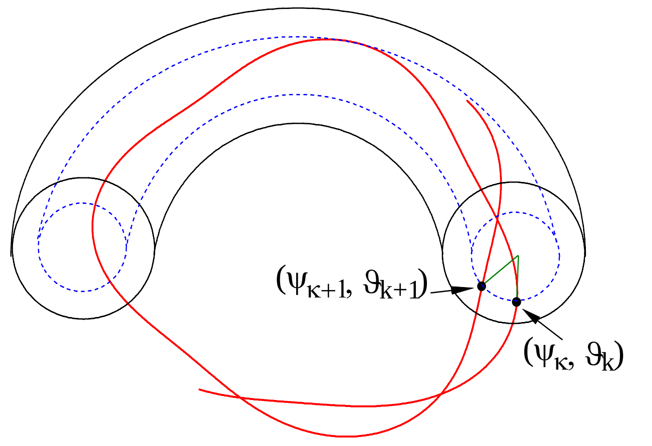

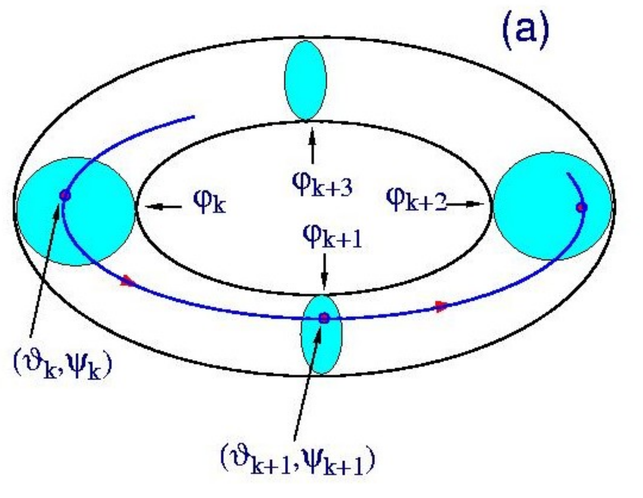

Poincaré plots

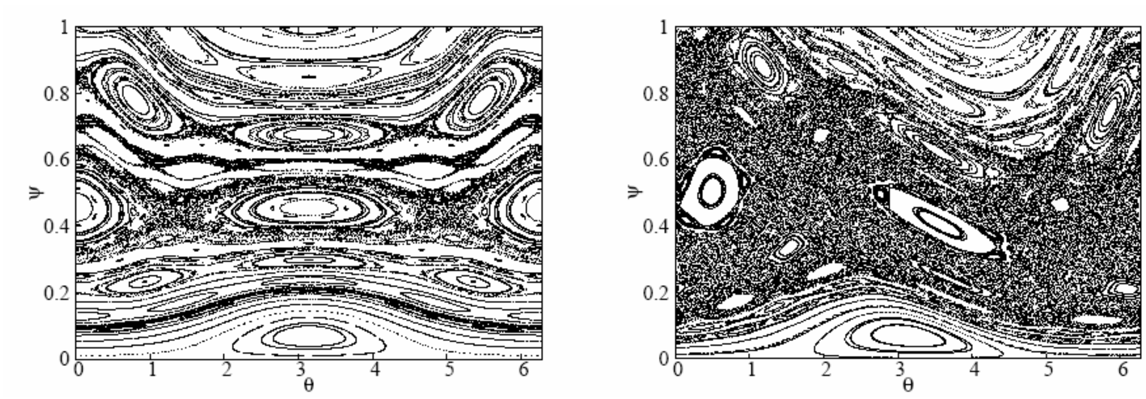

Comparison of correct symplectic (left) versus non-symplectic (right) map

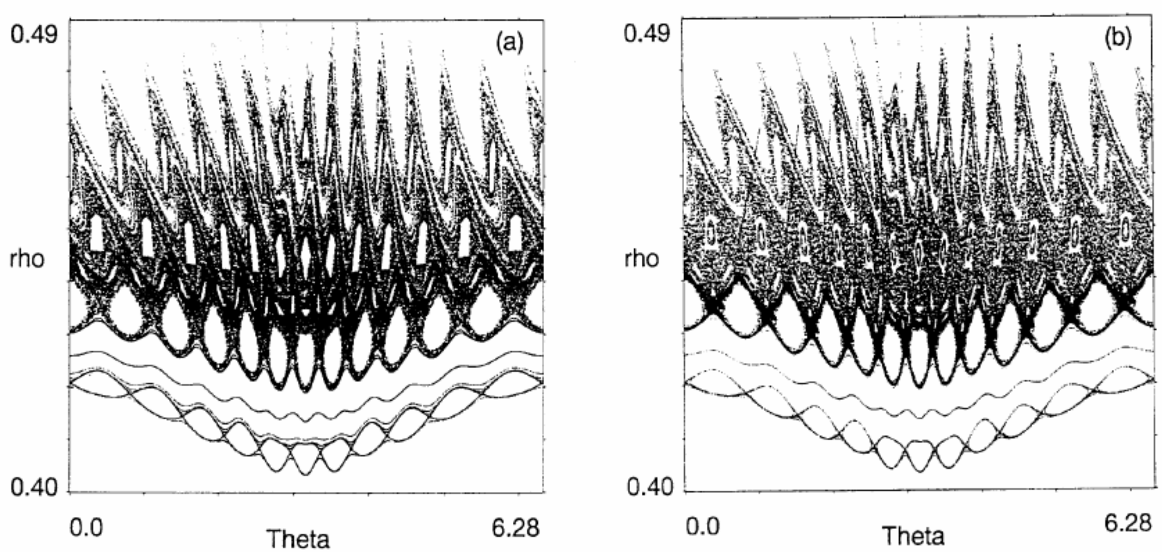

Comparison of Poincaré plots: Field line tracing (left) versus symplectic map (right)

Characterization of chaotic systems

$$(\vartheta_{k+1},\psi_{k+1}) = \hat{M}(\vartheta_k,\psi_k)$$

$$d\vec{I}_k = \begin{pmatrix} d\psi_k \\ d\vartheta_k \end{pmatrix} \;,\; d\vec{I}_{k+1} = J_k d\vec{I}_k \;,\; J_k = \begin{pmatrix} \dfrac{\partial\psi_{k+1}}{\partial\psi_k} & \dfrac{\partial\psi_{k+1}}{\partial\vartheta_k} \\ \dfrac{\partial\vartheta_{k+1}}{\partial\psi_k} & \dfrac{\partial\vartheta_{k+1}}{\partial\vartheta_k} \end{pmatrix}$$

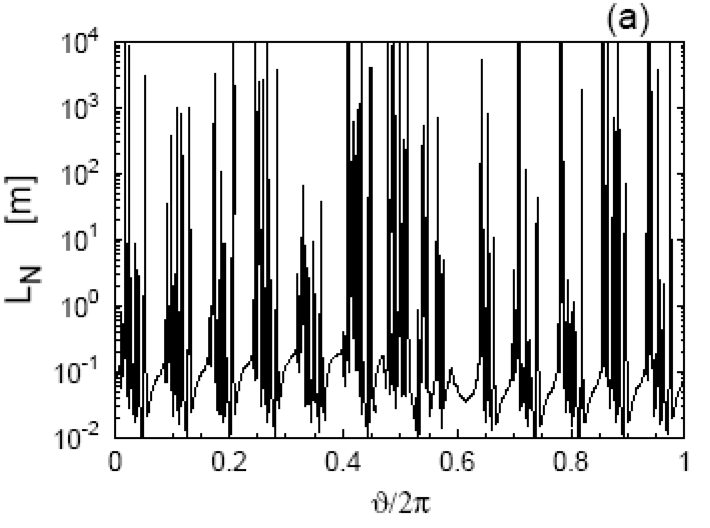

$$\begin{vmatrix} \dfrac{\partial\psi_{k+1}}{\partial\psi_k}-\lambda & \dfrac{\partial\psi_{k+1}}{\partial\vartheta_k} \\ \dfrac{\partial\vartheta_{k+1}}{\partial\psi_k} & \dfrac{\partial\vartheta_{k+1}}{\partial\vartheta_k}-\lambda \end{vmatrix} = 0 \;,\; \lambda^{(k)} = \max(\lambda_1^{(k)},\lambda_2^{(k)})$$

$\sigma = \lim\limits_{N\to\infty}\dfrac{1}{N}\ln\prod\limits_{k=1}^{N}\lambda^{(k)} > 0$ [global Lyapunov exponent for unstable orbits]

$\sigma_N = \dfrac{1}{N}\ln\prod\limits_{k=1}^{N}\lambda^{(k)} > 0$ [finite-time Lyapunov exponent for finite connection lengths]

$L_N = \dfrac{l}{\sigma_N}$ [local e-folding length, l length of field line per one map step]

Characterization of chaotic systems

$$(\vartheta_{k+1}, \psi_{k+1}) = \hat{M}(\vartheta_k, \psi_k)$$

Kolmogorov length

$$L_K(\rho, N) = \bar{L}_N = \frac{l}{\bar{\sigma}_N} \quad \text{[averaged over magnetic surface of radius } \rho\text{]}$$

$$\approx \pi q R_0 \left(\frac{\pi \sigma_{Chir}}{2} \right)^{-4/3} \quad \text{[quasi-classical approximation]}$$

$$\langle |\Delta \vec{x}_\perp(\zeta)|^2 \rangle \sim |\Delta \vec{x}_\perp(0)|^2 \ \exp\left\{ \frac{2\zeta}{L_K} \right\}$$

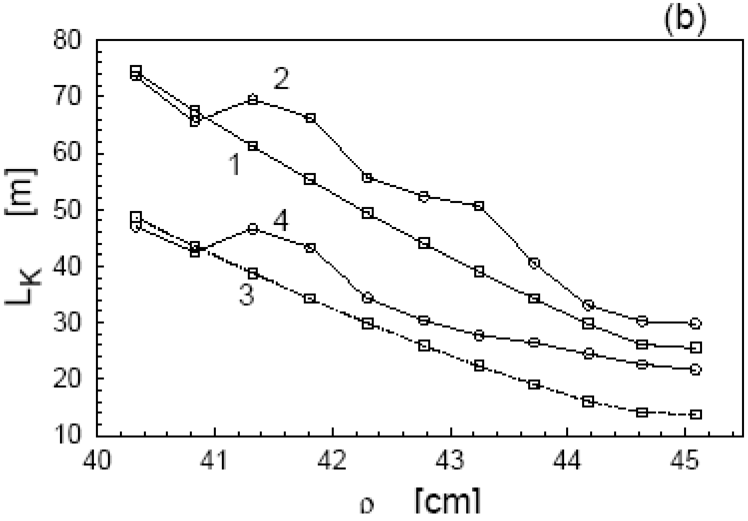

(Open) chaotic scattering system

Connection lengths → Laminar plots

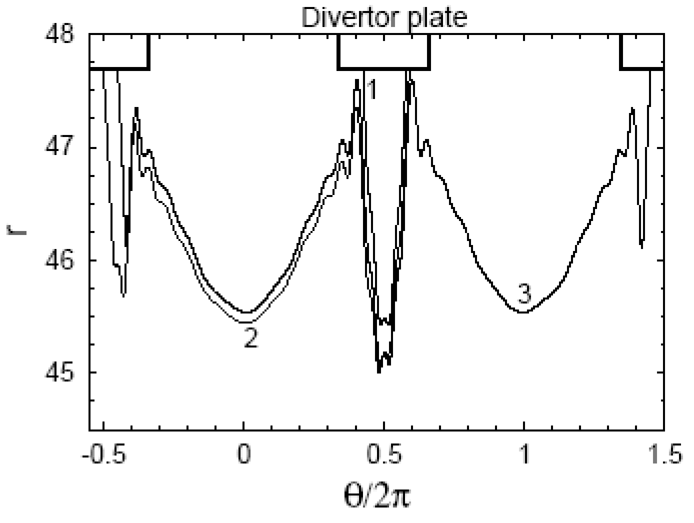

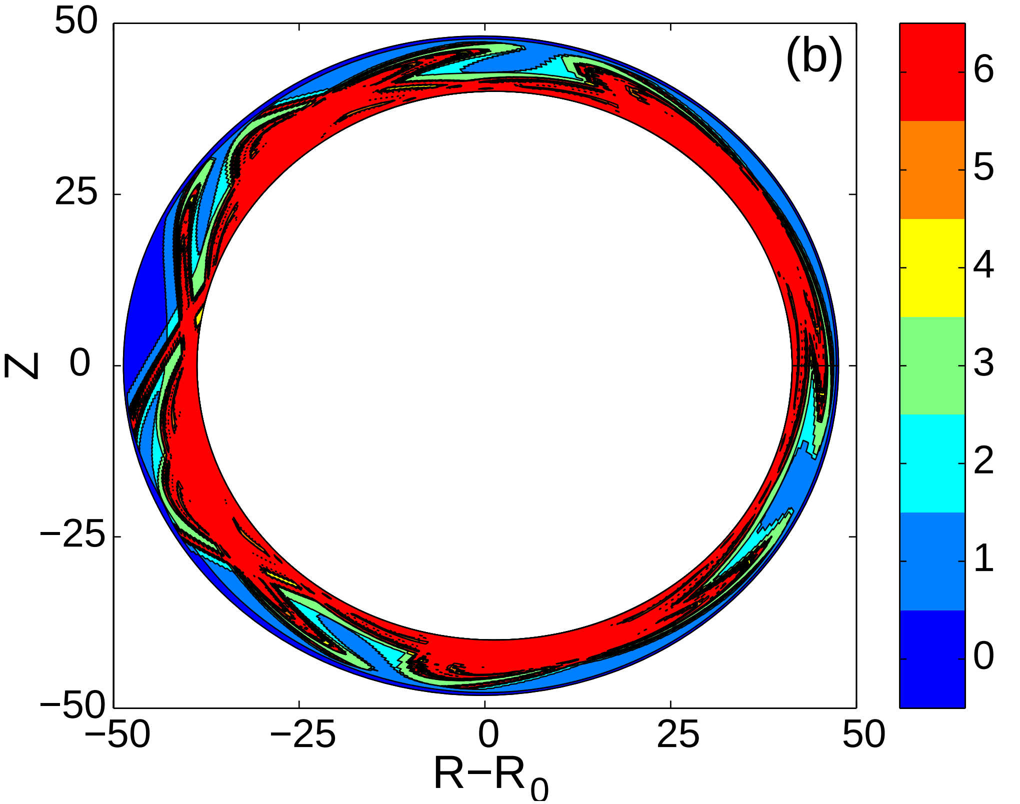

CIII emission spectrum and field line structure

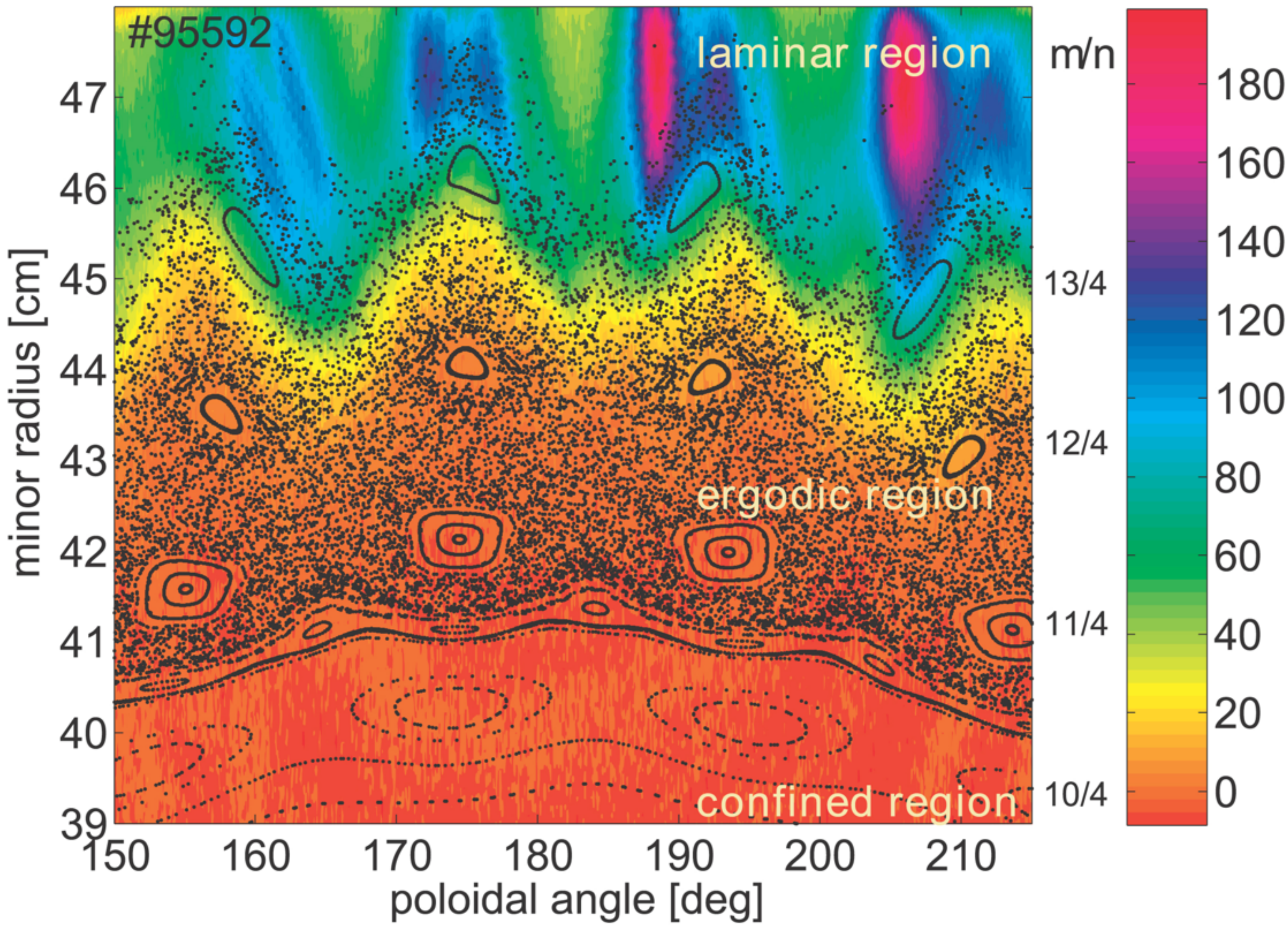

Laminar region: Connection length < Kolmogorov length

Quasi-linear field line diffusion

$$\frac{d\psi}{d\zeta} = -\frac{\partial \Psi_p}{\partial \theta}, \qquad \frac{d\theta}{d\zeta} = \frac{\partial \Psi_p}{\partial \psi}$$

$$H \equiv \Psi_p = H_0(\psi) + \varepsilon H_1(\theta,\psi,\zeta) \;\;,\;\; V_1 = -\frac{\partial H_1}{\partial \theta}$$

$$\frac{df}{dt} = \frac{\partial f}{\partial \zeta} + \dot{\theta}\frac{\partial f}{\partial \theta} + \dot{\psi}\frac{\partial f}{\partial \psi} = \frac{\partial f}{\partial \zeta} + \frac{\partial H}{\partial \psi}\frac{\partial f}{\partial \theta} - \frac{\partial H}{\partial \theta}\frac{\partial f}{\partial \psi}$$

$$\frac{\partial \bar{f}_0}{\partial \zeta_2} = \frac{\partial}{\partial \psi}\left(D \frac{\partial \bar{f}_0}{\partial \psi} \right)$$

$$D \equiv D(\psi) = \left\langle \int_0^{\zeta_0} d\zeta_0' V_1\left[\theta - \Omega\zeta_0', \psi, \zeta_0 - \zeta_0'\right] V_1\left[\theta, \psi, \zeta_0\right] \right\rangle_{\theta,\zeta_0}$$

Magnetic diffusion coefficient

$$D_{m(agnetic)} = \int_0^\infty d\zeta \, \langle b_x[\vec{x}_\perp(\zeta),\zeta] \, b_x[\vec{x}_\perp(0),0] \rangle \sim b^2 \, L_{corr}$$

$$\Delta x < \lambda_\perp : \;\; D_m \lambda_\parallel < \lambda_\perp^2 \to L_{corr} \approx \lambda_\parallel \to D_m \approx b^2 \lambda_\parallel$$

$$\Delta x > \lambda_\perp : \;\; D_m \lambda_\parallel > \lambda_\perp^2 \to D_m \, L_{corr} \approx \lambda_\perp^2 \to D_m \approx \frac{b^2 \lambda_\perp^2}{D_m} \to D_m \approx b \lambda_\perp$$

$$D_m \approx \begin{cases} b^2 \lambda_\parallel & \text{for} \quad \text{b} < \dfrac{\lambda_\perp}{\lambda_\parallel} \\ b \lambda_\perp & \text{for} \quad \text{b} > \dfrac{\lambda_\perp}{\lambda_\parallel} \end{cases}$$

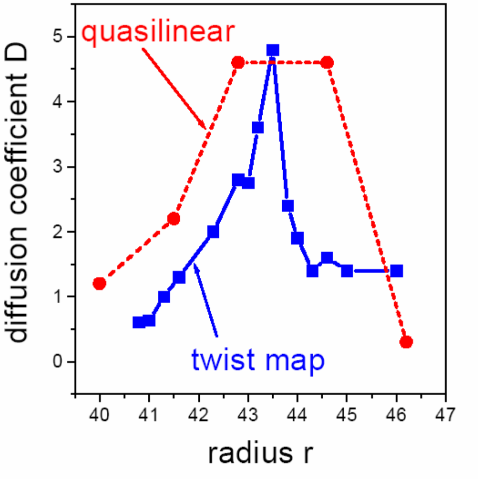

Results without trapping:

$D_m \approx b^2 \lambda_\parallel$ (for $\lambda_\perp \to \infty$) [quasilinear]

$D_m \approx b \; \lambda_\perp$ (for $\lambda_\parallel \to \infty, \lambda_\perp$ finite) [Kadomtsev-Pogutse] trapping?

Non-diffusive transport in the presence of hyperbolic fixed points

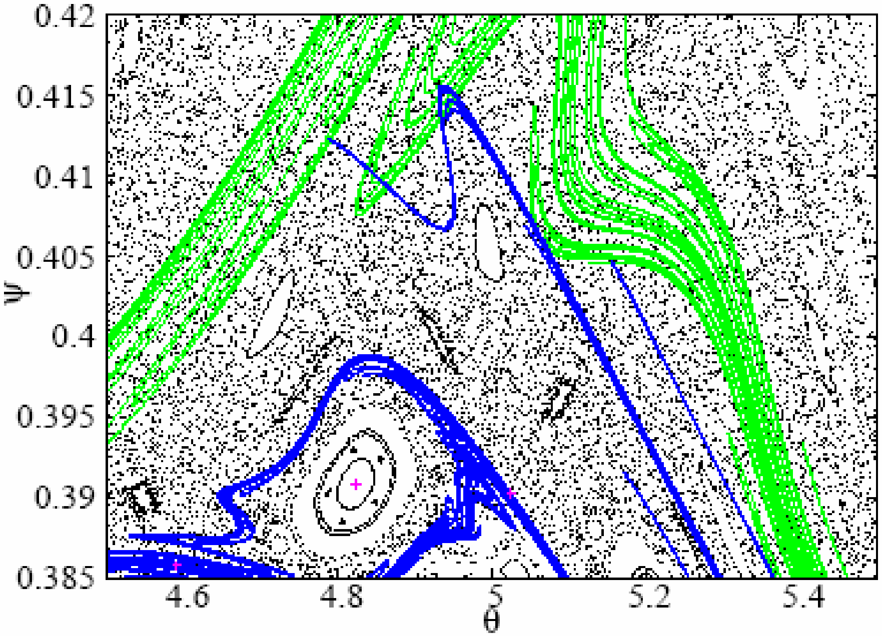

Stable and unstable manifolds of periodic hyperbolic fixed points

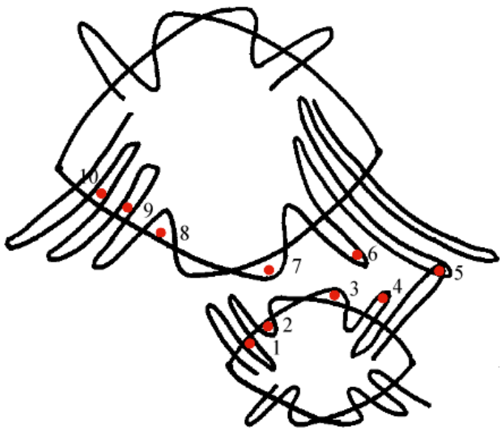

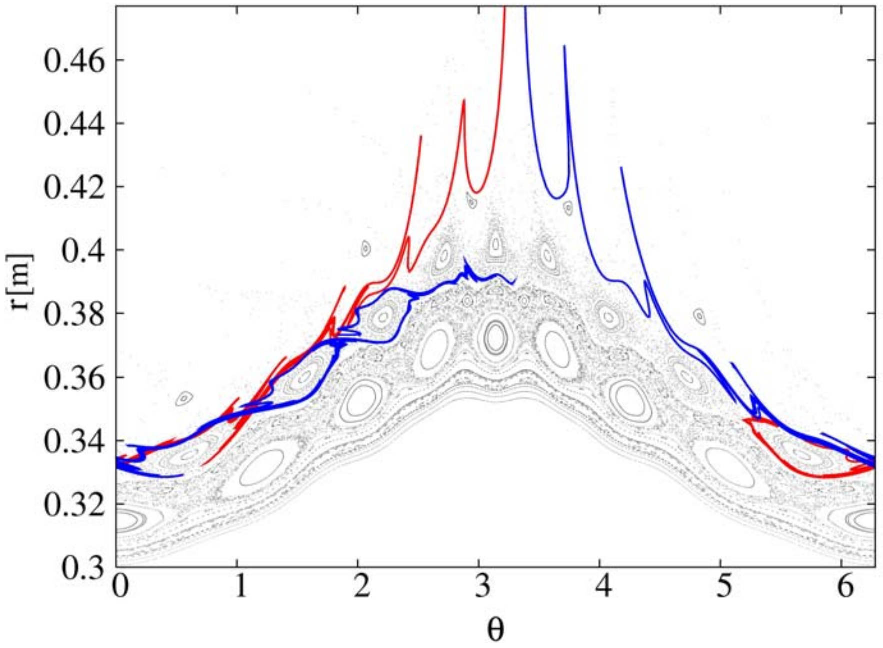

Heat deposition pattern

Laminar plots versus manifold strike points (see also the MASTOC criterion)

Experiment:

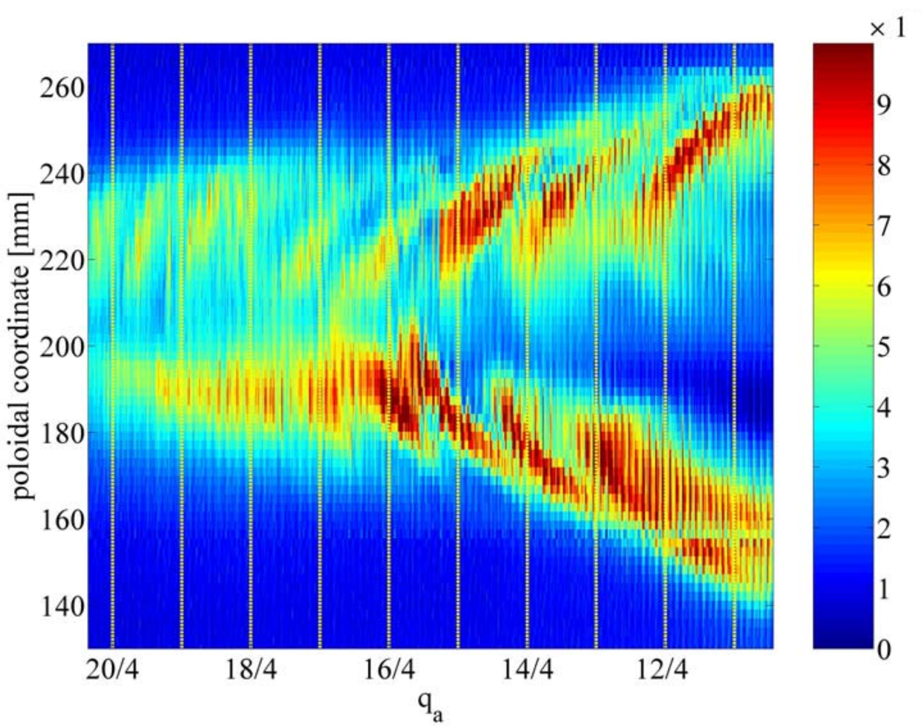

Theory:

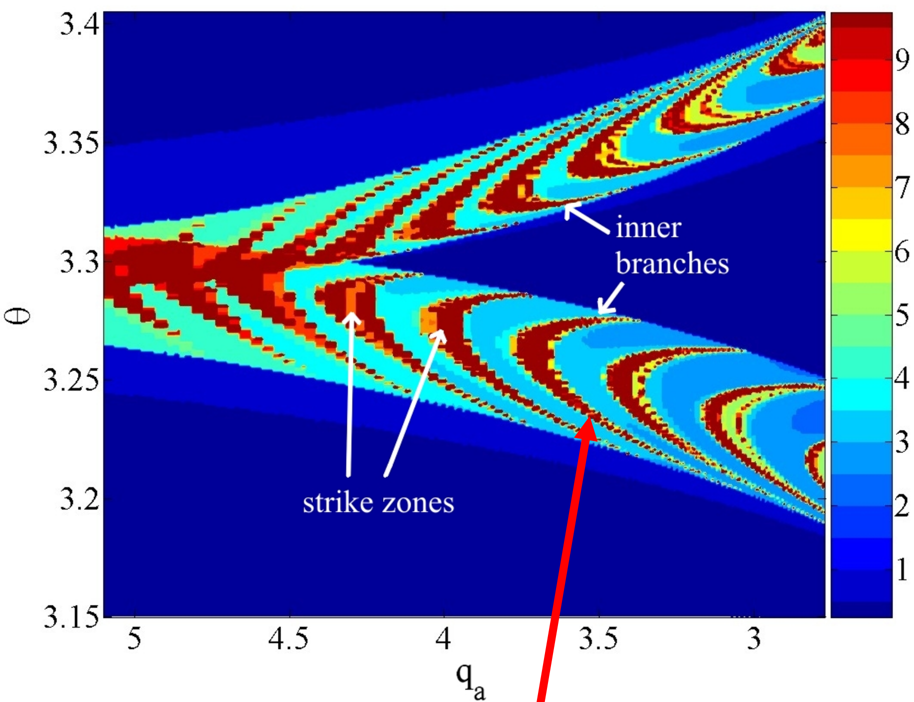

q – profile at the edge: $$q_a = \frac{2\pi B_0 a^2}{\mu_0 R_0 I_p}$$

Manifolds select outer strike zones

Ab initio theory: A-Langevin equation model

Monte-Carlo-simulation

$$\dot{\boldsymbol{u}}(t) = \frac{Z\,e}{m\,c}\,\boldsymbol{u}(t)\times\boldsymbol{B}(t) - \nu\,\boldsymbol{u}(t) + \boldsymbol{a}(t)$$

$$\boldsymbol{B} = B_0\,(b_0\,\boldsymbol{e}_z + \boldsymbol{b})$$

Velocity

DCT, Corrsin

Lagrangian correlator+Green-Kubo-formalism:
ODE for **diffusion coefficient**

V-Langevin approach (Balescu and co-workers)

Guiding center approach

$$\frac{dx_p(t)}{dt} = b_x[x_p(t), y_p(t), z_p(t)]\frac{dz_p(t)}{dt} + \eta_{\perp x}(t)$$

$$\frac{dy_p(t)}{dt} = b_y[x_p(t), y_p(t), z_p(t)]\frac{dz_p(t)}{dt} + \eta_{\perp y}(t)$$

$$\frac{dz_p(t)}{dt} = \eta_{||}(t)$$

Trapping and finite Larmor radii

Trapping

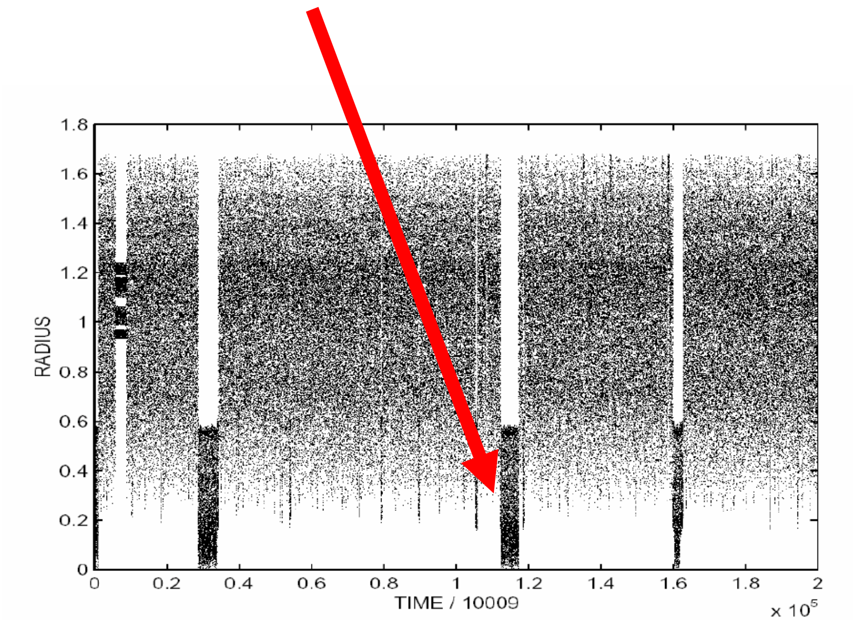

Comparison: island width $w_{m,n}$

$$w_{m,n} = \Lambda(\theta)\left|\frac{r_{m,n} b_{r(m,n)} q_{m,n}}{m b_\theta \, \partial q_{m,n} / dr}\right|^{1/2} \sim \sqrt{b_{r(m,n)}}$$

and Larmor radius ρ

Radial position of one trajectory

$$\dot{\boldsymbol{u}}(t) = \frac{Z e}{m c} \boldsymbol{u}(t) \times \boldsymbol{B}(t) - \nu \boldsymbol{u}(t) + \boldsymbol{a}(t)$$

$$\boldsymbol{B} = B_0 \left(b_0 \boldsymbol{e}_z + \boldsymbol{b}\right)$$

Statistical physics of field line diffusion

Taylor-Green-Kubo formula: $D = \frac{\langle \vec{x}^2 \rangle}{2td} = \frac{1}{d}\int_0^\infty d\tau \ \langle \vec{v}[\vec{x}(\tau),\tau]\cdot\vec{v}[0,0]\rangle$

Lagrange correlation

$$D_{m(agnetic)} = \int_0^\infty d\zeta \ \langle b_x[\vec{x}_\perp(\zeta),\zeta]\ b_x[\vec{x}_\perp(0),0]\rangle \sim b^2 L_{corr}$$

$$L_{rs}(\zeta) = \langle b_r[\vec{x}_\perp(\zeta),\zeta]\ b_s[\vec{x}_\perp(0),0]\rangle$$

$$B_{mn} = \langle b_m[\vec{x}+\vec{r}]\ b_n[\vec{x}]\rangle \approx \beta^2\left[\left(1-\frac{r_\perp^2}{\lambda_\perp^2}\right)\delta_{mn} + \frac{r_m r_n}{\lambda_\perp^2}\right]\exp\left\{-\frac{z^2}{2\lambda_\parallel^2} - \frac{r_\perp^2}{2\lambda_\perp^2}\right\}$$

Corrsin: $L_{rs}(\zeta) \approx \int d^2 r_\perp \ B_{rs}(\vec{r}_\perp,\zeta)\ \left\langle \delta(\vec{r}_\perp - \vec{x}_\perp(\zeta))\right\rangle$

$$L(\zeta) \approx \beta^2 e^{-\zeta^2/2\lambda_\parallel^2}\ \frac{\lambda_\perp^4}{\left[\lambda_\perp^2 + 2\int_0^\zeta d\zeta'\,(\zeta-\zeta')L(\zeta')\right]^2}$$

$$D_m \approx \begin{cases} b^2\lambda_\parallel & \text{for } \lambda_\perp \to \infty \\ b\lambda_\perp & \text{for } \lambda_\parallel \to \infty \end{cases}$$

Quasilinear particle diffusion properties

$$\sigma^2 = 2D_{particle}\, t^{\gamma} \ ; \ \gamma = 1 \text{ diffusive}$$

$\perp$ non-diffusive (|| diffusive, no deviation from magnetic field line)

$$\sigma^2 = 2D_{magnetic}\, z \ , \quad z^2 \approx 2\chi_{\|} t \ , \ \sigma^2 = 2D_{magnetic}\sqrt{2\chi_{\|} t} \ \rightarrow \ \frac{\sigma^2}{t} \sim \frac{1}{\sqrt{t}} \xrightarrow[t\to\infty]{} 0$$

Quasilinear particle diffusion (Jokipii & Parker)

$$D_{\perp\ particle} \sim \frac{\left\langle (\Delta x)^2 \right\rangle}{\Delta t} \approx \frac{D_{magnetic}\ \lambda_{\|}}{\lambda_{\|} / \mathrm{v}_{thermal}} = D_{magnetic}\ \mathrm{v}_{thermal} \approx \beta^2 \lambda_{\|}\ \mathrm{v}_{thermal} \quad \text{[collisionless]}$$

$$D_{\perp\ particle} \sim \frac{\left\langle (\Delta x)^2 \right\rangle}{\Delta t} \approx \begin{cases} D_{magnetic} \dfrac{L_{corr}}{\tau_c} \approx \beta^2 \lambda_{\|}^2\, v_{collision} \sim \beta^2\ D_{\|\ particle} \\ \text{[collisional fluid limit, } \lambda_{\|} \approx L_{corr} \approx \mathrm{v}_{thermal} / v_{collision}\text{]} \\ \qquad \ldots \end{cases}$$

see more during ab initio calculations!

Rechester-Rosenbluth („oversimplified“)

$$\left\langle \left(\Delta x\right)^2 \right\rangle_l \approx \beta^2 \lambda_{\|} L_K$$

decorrelation time: $t_l \approx \dfrac{L_K^2}{\chi_{\|}}$

$$D_{particle} \approx \frac{\left\langle \left(\Delta x\right)^2 \right\rangle_l}{t_l}$$

$$D_{particle} \approx \frac{\beta^2 \lambda_{\|} \chi_{\|}}{L_K}$$

Rechester-Rosenbluth coefficient (weakly collisional)

$$\lambda_{mfp} \ll L_K < L_{diffusion}$$

$$\left\langle (\Delta x)^2 \right\rangle_{L_K} \approx \chi_\perp T_{L_K} = \chi_\perp \frac{L_K^2}{\chi_\parallel} \text{ with } \chi_\perp = \frac{\nu^2}{\Omega^2}\chi_\parallel \;,\quad \chi_\parallel = \frac{v_{th}^2}{2\nu}\;,\quad \nu T_{L_K} > 1$$

$$\text{magnetic field separation: } \lambda_\perp^2 \doteq \left\langle (\Delta x)^2 \right\rangle_{L_K} \exp\left\{\frac{2L_{diffusion}}{L_K}\right\} \rightarrow L_{diffusion} \approx L_K \ln\left(\frac{\lambda_\perp}{\sqrt{\left\langle (\Delta x)^2 \right\rangle_{L_K}}}\right)$$

$$\left\langle (\Delta x)^2 \right\rangle_{L_{diffusion}} \approx D_m L_{diffusion} \;,\; D_{particle} \approx \frac{\left\langle (\Delta x)^2 \right\rangle_{L_{diffusion}}}{\dfrac{L_{diffusion}^2}{\chi_\parallel}}$$

$$\boxed{D_{particle}^{RR} \approx \frac{D_m \chi_\parallel}{L_K \ln\left(\dfrac{\lambda_\perp}{L_K}\sqrt{\dfrac{\chi_\parallel}{\chi_\perp}}\right)}} \sim \frac{D_m \chi_\parallel}{L_K} \sim \chi_\parallel \beta^2 K^2 \text{ with } K \approx \frac{\beta \lambda_\parallel}{\lambda_\perp} \text{ and } L_K \approx \sqrt{\frac{2}{\pi}}\frac{\lambda_\perp^2}{4\beta^2\lambda_\parallel}$$

Kadomtsev-Pogutse coefficient (strongly collisional)

$$\left\langle (\Delta x)^2 \right\rangle_l \approx \beta^2 \lambda_{\parallel} l \quad \text{with } l^2 \approx \chi_{\parallel} t_l$$

decorrelation time: $t_l \approx \dfrac{\lambda_{\perp}^2}{\chi_{\perp}}$

$$D_{particle} \approx \frac{\left\langle (\Delta x)^2 \right\rangle_l}{t_l}$$

$$\boxed{D_{particle} \approx \frac{\beta^2 \lambda_{\parallel}}{\lambda_{\perp}} \sqrt{\chi_{\parallel} \chi_{\perp}}} \sim \beta K D_{Bohm}$$

with $K \approx \dfrac{\beta \lambda_{\parallel}}{\lambda_{\perp}}$ and $D_{Bohm} \approx \dfrac{1}{16} \sqrt{\chi_{\parallel} \chi_{\perp}} \sim \dfrac{cT}{eB}$

Comparison (simplified)

Rechester-Rosenbluth:

$$\left\langle (\Delta x)^2 \right\rangle_{L_K} \approx D_m\, L_K = D_{particle}\, T_K$$

$$T_K \approx \frac{L_K^2}{\chi_{||}}$$

$$D_{particle}^{RR} \approx \frac{\beta^2 \lambda_{||} \chi_{||}}{L_K} \sim \frac{\beta^4 \lambda_{||}^2 \chi_{||}}{\lambda_{\perp}^2}$$

$$T_K \ll t_l : \qquad \boxed{\nu < \Omega \beta K}$$

Kadomtsev-Pogutse:

$$\left\langle (\Delta x)^2 \right\rangle_{l_{coll}} \approx D_m\, l_{coll} = D_{particle}\, t_l$$

$$t_l \approx \frac{l_{coll}^2}{\chi_{||}}\,, \quad t_l \approx \frac{\lambda_{\perp}^2}{\chi_{\perp}} \rightarrow l_{coll} \approx \sqrt{\frac{\chi_{||}}{\chi_{\perp}}}\, \lambda_{\perp}$$

$$D_{particle}^{KP} \approx \frac{\left\langle (\Delta x)^2 \right\rangle_l}{t_l} \approx \frac{\beta^2 \lambda_{||}}{\lambda_{\perp}} \sqrt{\chi_{||} \chi_{\perp}}$$

$$T_K \gg t_l : \qquad \boxed{\nu > \Omega \beta K}$$

Running diffusion coefficient for K<1 (Langevin theory)

Parameters: ν, $\lambda_\parallel$, $\lambda_\perp$, β, Ω

$D \sim \beta^2 \lambda_\parallel v_{th} \sim K$ (Jokipii&Parker) or $D \sim \beta^2 \chi_\parallel$ (fluid) or $\chi_\parallel$ $(\beta \to 0, \nu \neq 0)$

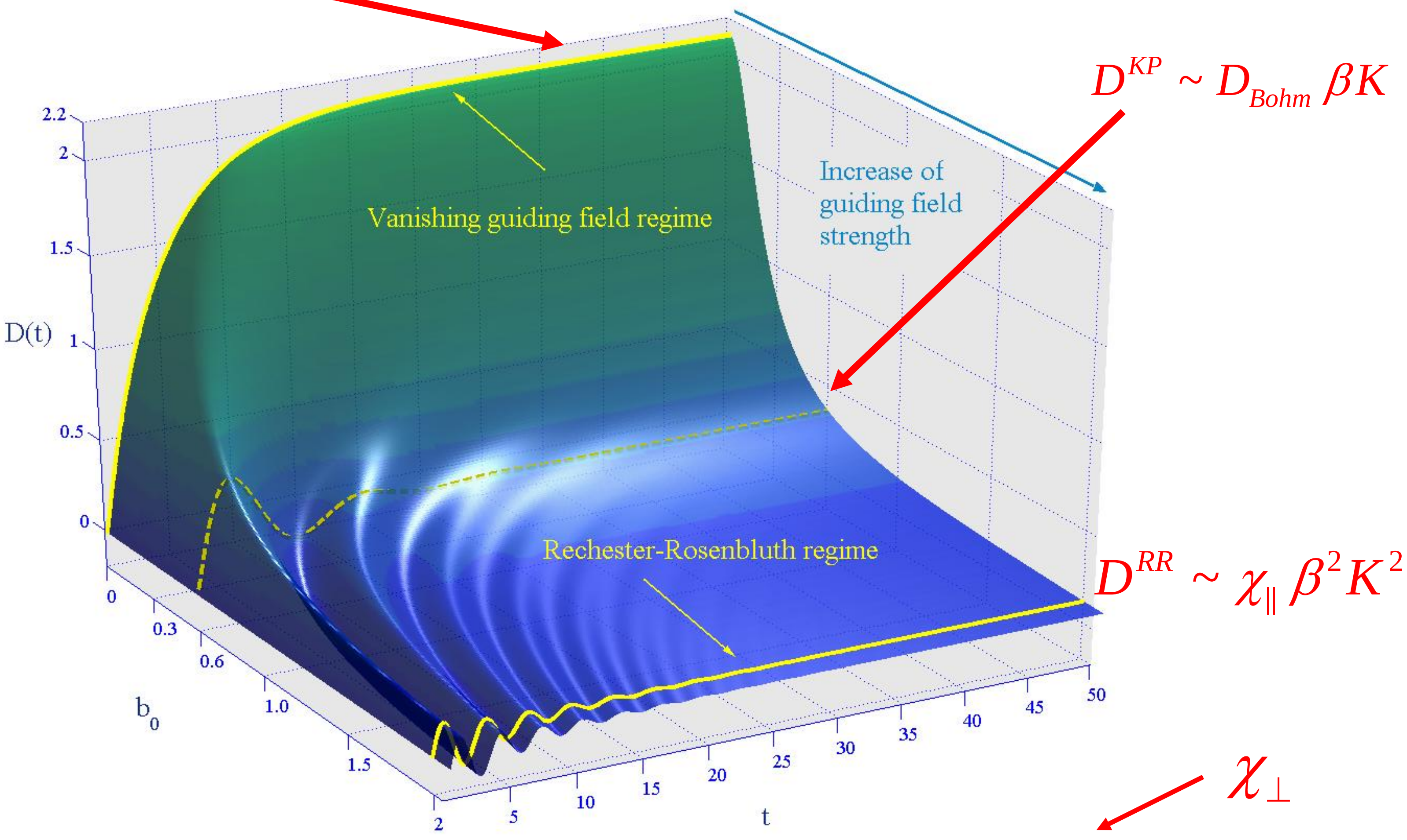

Finite Larmor radius effects for K<1

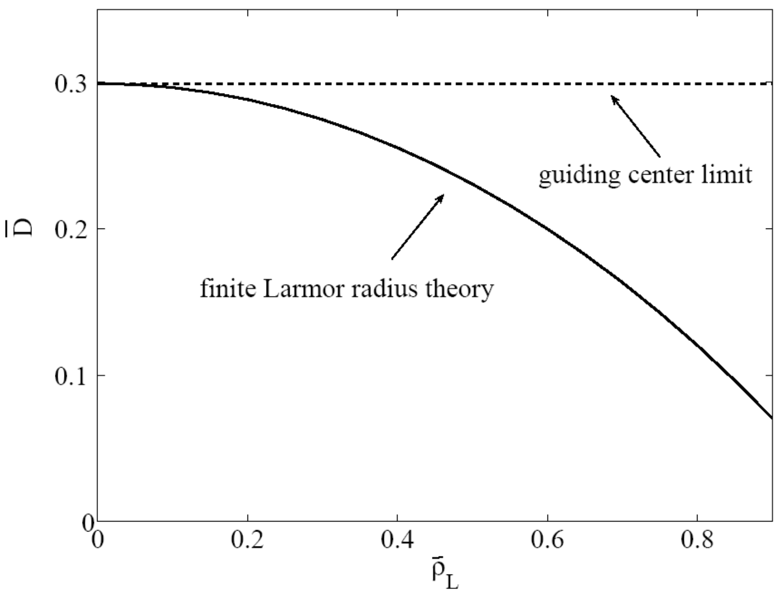

Finite Larmor radii decorrelate the particles from exponentially diverging magnetic field lines

Monte Carlo simulations support the analytical predictions

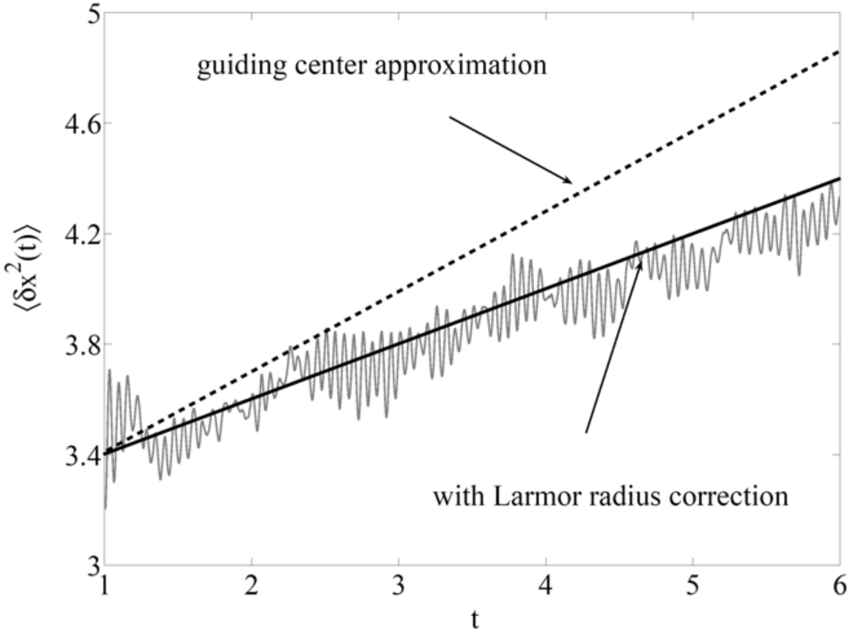

The role of large Kubo numbers

$$\boldsymbol{b}(\boldsymbol{x}, z) = \nabla\phi(\boldsymbol{x}, z) \times \boldsymbol{e}_z$$

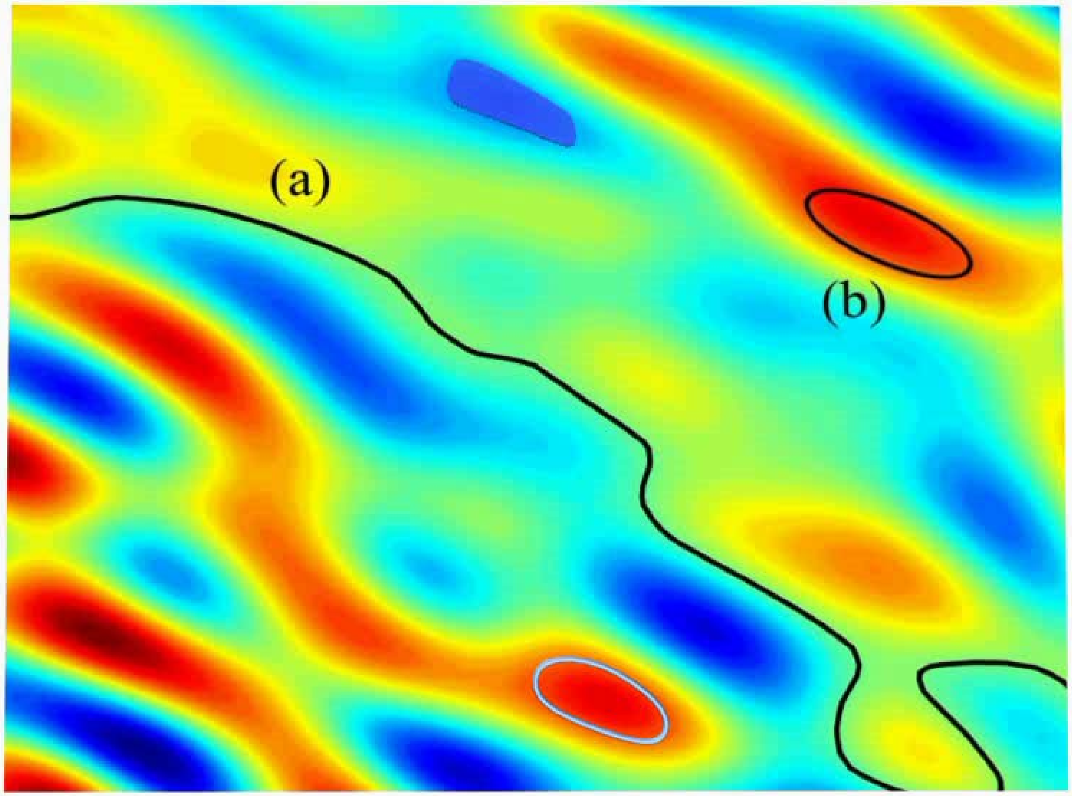

Kubo number K:

$$K = \frac{V\tau_C}{\lambda_C}$$

$$K \approx \frac{\beta\,\lambda_\parallel}{\lambda_\perp} \leq 1\text{: Corrsin}$$

$K \gg 1$: DCT

Trapping

Percolation

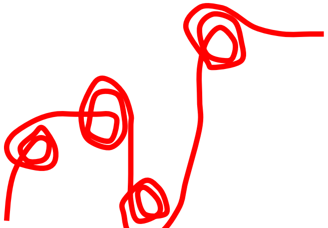

Percolation limit K>>1

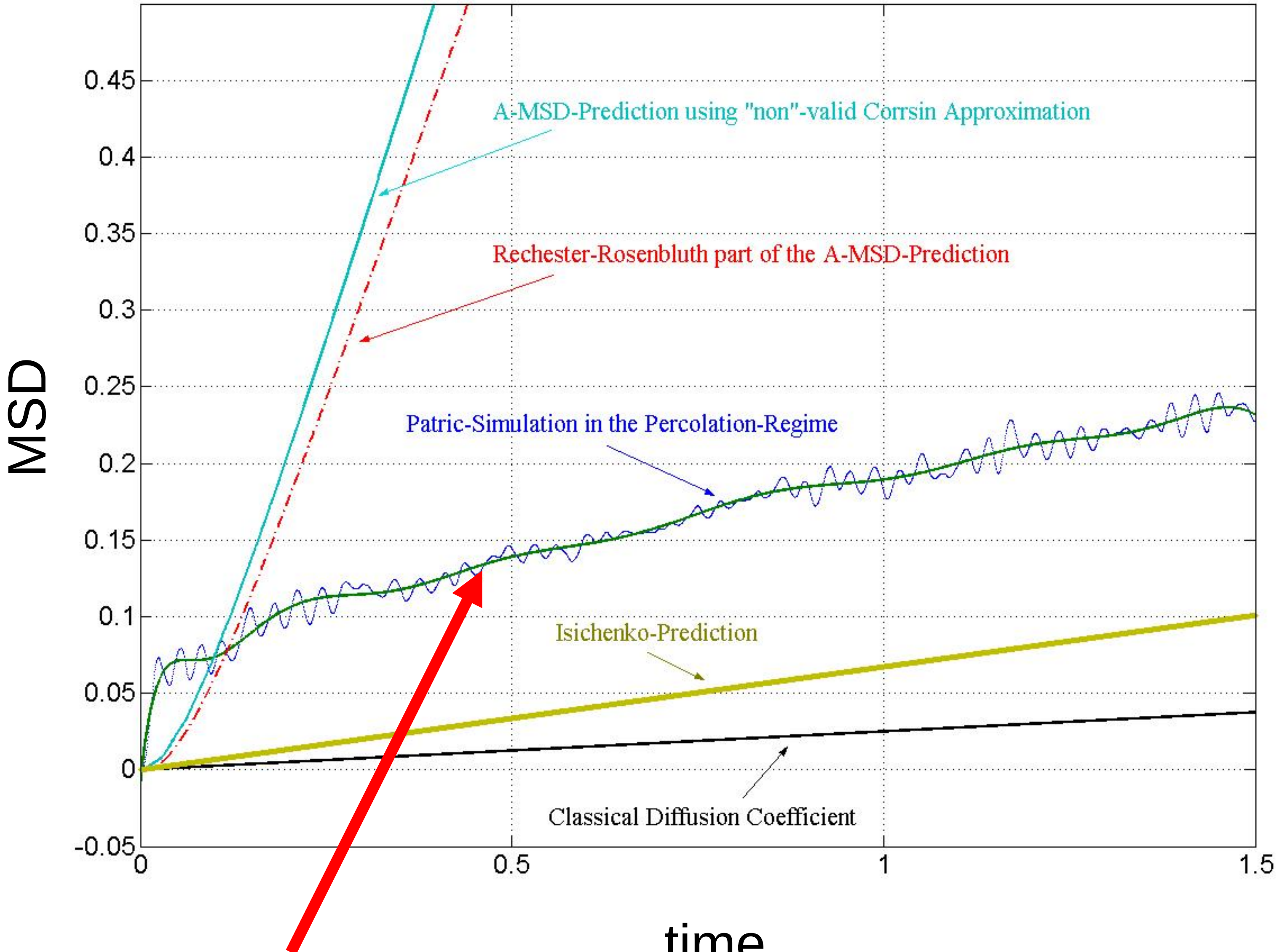

$D \sim 1/K^{07}$

D → 0 in the percolation limit K>>1

naive (wrong!) argument: $\lambda_{\|} \to \infty : D_{magnetic} \sim \beta\lambda_{\perp} \sim K^0$

$$\frac{dx}{dz} = \frac{b_x^{trapping} + b_x^{random}}{B_0} \;,\quad \frac{dy}{dz} = \frac{b_y^{trapping} + b_y^{random}}{B_0} \;,\quad \vec{b}^{trapping} = \nabla \times a\,\hat{z} \;,\quad a \approx A \exp\left\{-\frac{r^2}{2\sigma^2}\right\}$$

$$\frac{d^2x}{dz^2} \approx -\kappa^2 x \;,\quad \kappa = \frac{a}{B_0\sigma^2}$$

$$\langle \Delta r^2 \rangle = \frac{1}{B_0^2}\int\int dz'dz''\langle b_r^{random}(z')\, b_r^{random}(z'')\rangle \sim \frac{2z}{B_0^2} P_{xx}(\kappa)$$

with $P_{xx}(k) = \frac{1}{2\pi}\int B_{xx}(\Delta z)\exp\{-ik\Delta z\}d\Delta z$ since $b_r^{random}(z) \sim b_x^{random}(z)\cos(\kappa z)$

example: Kolmogorov spectrum $P_{xx}(k) \approx \dfrac{C}{\left[1+\left(k\lambda_{\|}\right)^2\right]^{5/6}}$

$$D_{rr} \approx D^{quasilinear}\frac{P_{xx}(\kappa)}{P_{xx}(0)} \sim \begin{cases} D^{quasilinear} & \text{for } \kappa\lambda_{\|} \ll 1 \\ \kappa^{-5/3} \to 0 & \text{for } \kappa\lambda_{\|} \gg 1 \end{cases}$$

$$\kappa\lambda_{\|} = \frac{a\lambda_{\|}}{B_0\sigma^2} \sim \frac{a}{B_0\sigma}\frac{\lambda_{\|}}{\sigma} \sim \beta\frac{\lambda_{\|}}{\lambda_{\perp}} \sim K \text{ [Kubo number]}$$

DCT (decorrelation trajectory method)

$$Subensemble\ \phi(\vec{0},0)=\phi^0, \qquad \vec{v}(\vec{0},0)=\vec{v}^0$$

$$Lagrange\ correlator\ \ L_{ij}=\int d\phi^0 d\vec{v}^0 P(\phi^0,\vec{v}^0)\, v_i^0 \langle v_j(\vec{r}(t),t)\rangle^S$$

$$Eulerian\ mean\ velocity\ via\ conditional\ \ probability:$$

$$\langle v_j(\vec{r},t)\rangle^S=\left[\phi^0 E_{\phi j}(\vec{r})+v_x^0 E_{xj}(\vec{r})+v_y^0 E_{yj}(\vec{r})\right]\exp\left\{-\theta/K\right\}$$

$$\equiv f_j(\vec{r};\phi^0,\vec{v}^0)\exp\left\{-\theta/K\right\}, \qquad \theta\sim t$$

$$space-time\ decorrelation\ trajectory:$$

$$\frac{d}{dt}\vec{X}^S(t)=\vec{f}(\vec{X}^S;\phi^0,\vec{v}^0)\exp\left\{-\theta/K\right\}\equiv\vec{V}^S(\vec{X}^S(t),t), \qquad \vec{X}^S(t=0)=\vec{0}$$

$$L_{ij}=\int d\phi^0 d\vec{v}^0 P(\phi^0,\vec{v}^0)\, v_i^0 V_j^S(\vec{X}^S(t),t)$$

Finite Larmor radius effects

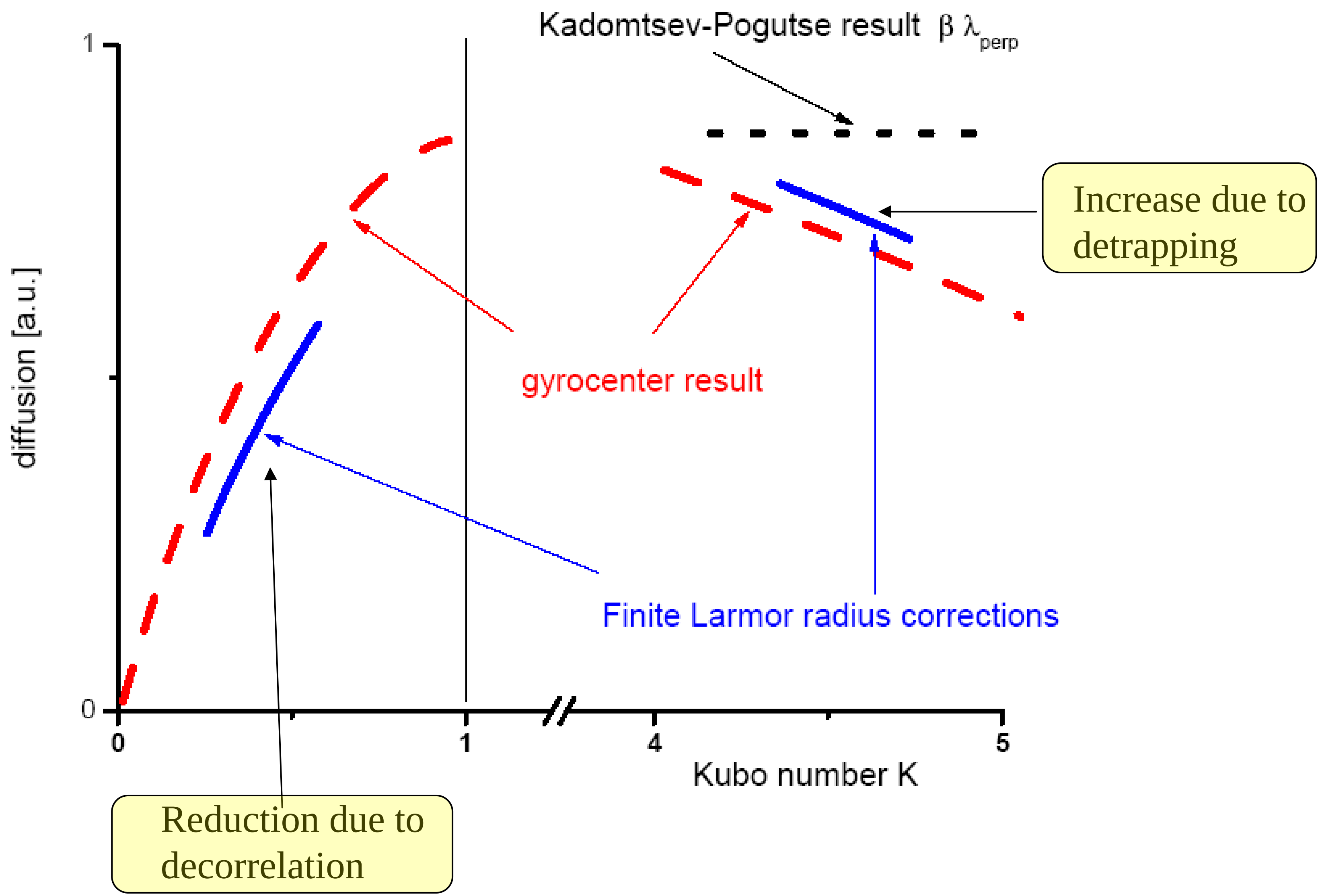

Large Kubo numbers K>>1

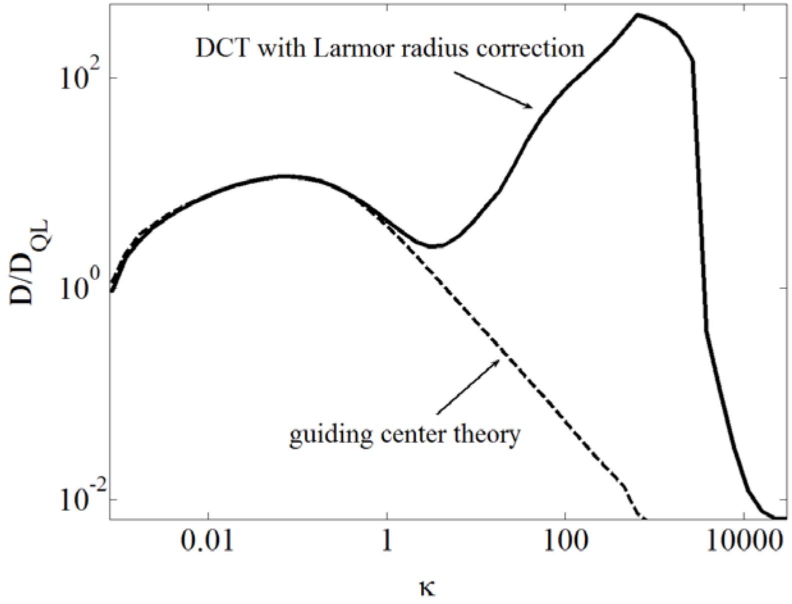

Finite Larmor radii
reduce the trapping effects
(collisionless case)

Collisions
reduce the trapping effects
(collisional cases)

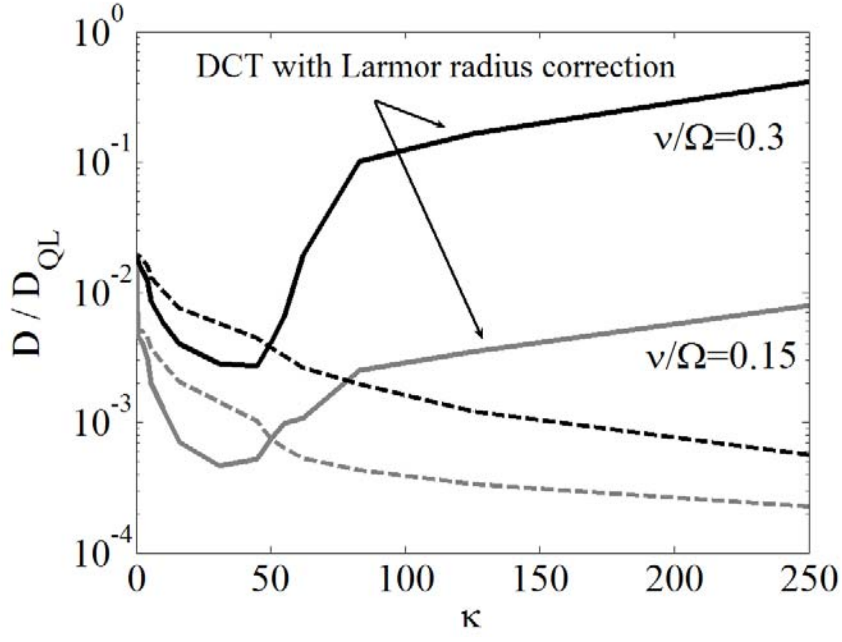

Percolative regime: Comparison with simulations

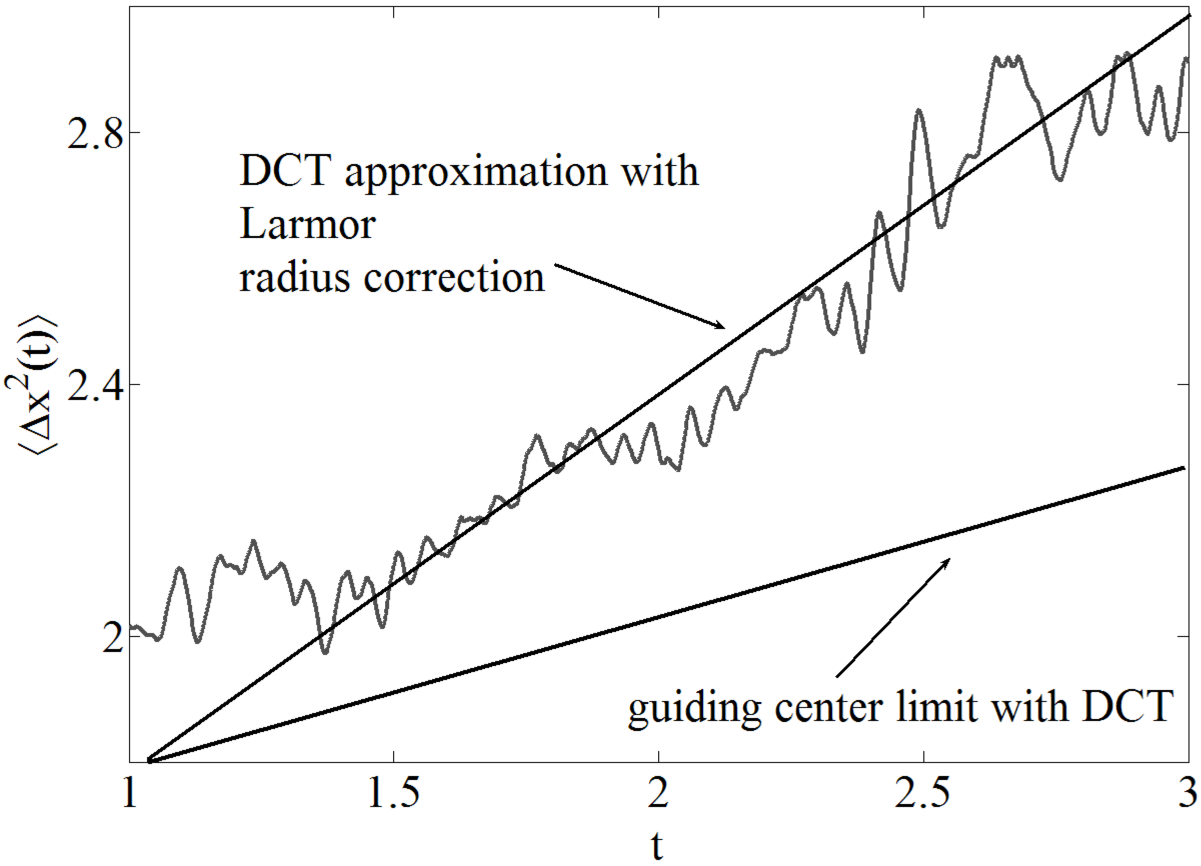

Parallel (pitch angle) diffusion

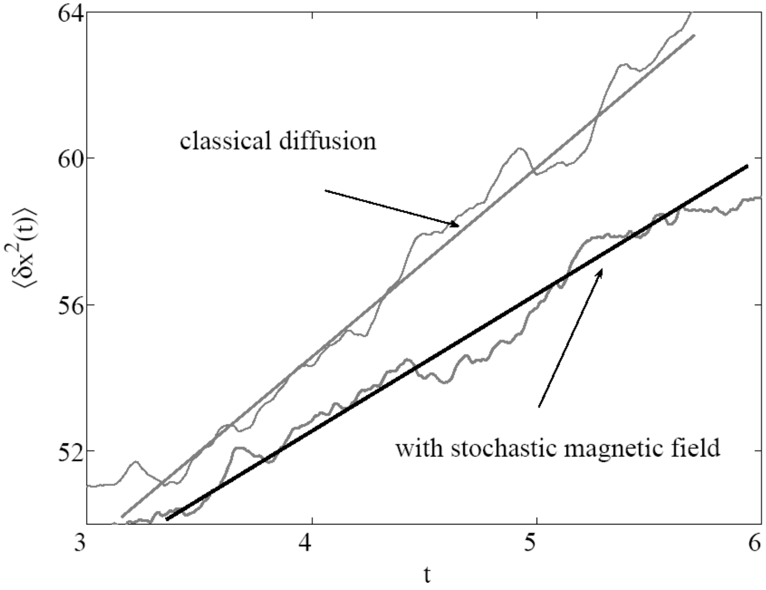

effective collision frequency:

$$\nu \rightarrow \nu + \nu_{fluctuation} \quad , \quad \beta = \frac{\delta B}{b_0}, \; \Omega = \frac{e b_0}{mc}$$

$$\nu_{fluctuation} \approx \beta^2 \frac{\lambda_{\parallel} \Omega^2}{v_{thermal}}$$

$\triangleq$ quasilinear

quasilinear
collisionless case
K<<1

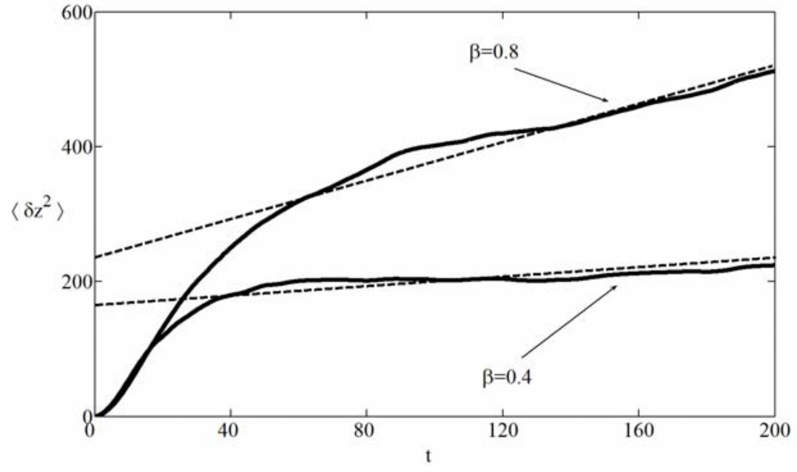

Parallel (pitch angle) diffusion

K >> 1

DCT versus Corrsin

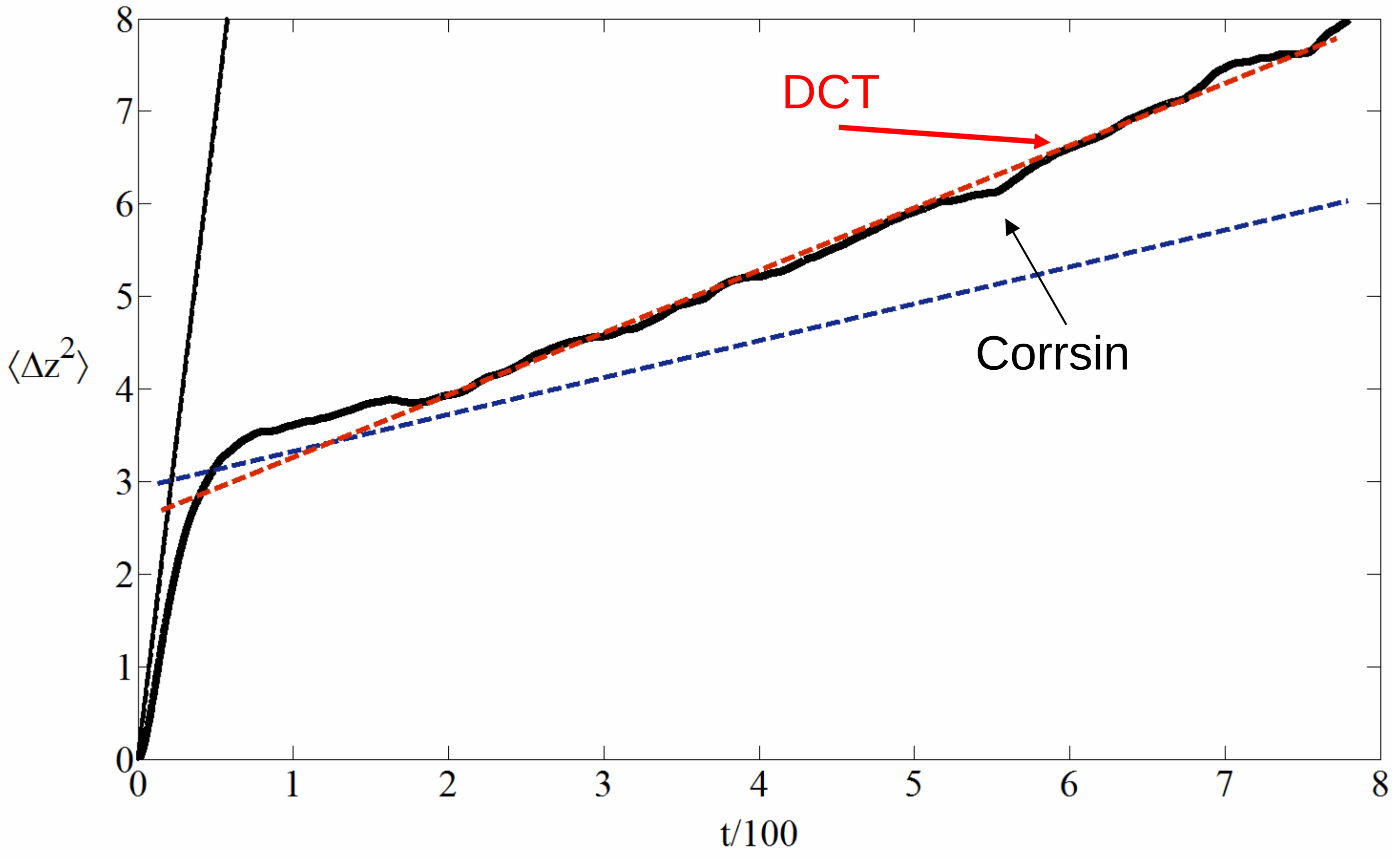

SUMMARY

Closures (beyond Corrsin) in the presence of structures (incomplete chaos) seem to work well

We have a quite complete picture of the parameter dependencies of stochastic transport coefficients

The qualitative as well as quantitative effects of stochastic transport should be further evaluated in dynamical models for ergodic divertors

Manageable stochasticity
• has many applications
• is a test basis for nonlinear plasma transport
• is ITER relevant

Thanks to many contributors
(Sadrilla Abdullaev, Andreas Wingen, Marcus Neuer,
Marcin Jakubowski, …)

Correct citations will appear in the written text!